Light-controlled inhibition of BRAFV600E kinase

Hoorens, Mark W H; Ourailidou, Maria E; Rodat, Theo; van der Wouden, Petra E; Kobauri, Piermichele; Kriegs, Malte; Peifer, Christian; Feringa, Ben L; Dekker, Frank J; Szymanski, Wiktor

Published in:
European Journal of Medicinal Chemistry

DOI:
10.1016/j.ejmech.2019.06.042

Publication date:
2019

Light-controlled Inhibition of BRAF^{V600E} Kinase

Mark W. H. Hoorens[1,2], Maria E. Ourailidou[3], Theo Rodat[4], Petra E. van der Wouden[3], Piermichele Kobauri[2], Malte Kriegs[5], Christian Peifer[4], Ben L. Feringa[2], Frank J. Dekker[3], Wiktor Szymanski[1,2]*

Affiliations

1: University Medical Center Groningen, Department of Radiology, Medical Imaging Center, University of Groningen, Hanzeplein 1, 9713 GZ Groningen, The Netherlands

2: Stratingh Institute for Chemistry, Faculty of Science and Engineering, University of Groningen, Nijenborgh 7, 9747 AG Groningen, The Netherlands

3: Department of Chemical and Pharmaceutical Biology, University of Groningen, Antonius Deusinglaan 1, 9713 AV Groningen, The Netherlands

4: Institute of Pharmacy, Christian-Albrechts-University of Kiel, Gutenbergstr. 76, 24118 Kiel, Germany

5: Laboratory of Radiobiology & Experimental Radiooncology and UCCH Kinomics Core Facility, University Medical Center Hamburg-Eppendorf, Martinistr. 52, 20246 Hamburg, Germany

Highlights

- Photochemical control over the inhibition of $BRAF^{V600E}$ kinase was achieved.

- Diaryl-sulfonamide motifs are promising targets for the azologization approach.

- Azologization of kinase inhibitors does not only alter their activity, but also their kinase selectivity.

Keywords

- $BRAF^{V600E}$

- Photopharmacology

- Photocontrolled inhibitor

- Metastatic melanoma

- Azobenzene

Abstract

Metastatic melanoma is amongst the most difficult types of cancer to treat, with current therapies mainly relying on the inhibition of the $BRAF^{V600E}$ mutant kinase. However, systemic inhibition of BRAF by small molecule drugs in cancer patients results – paradoxically – in increased wild-type BRAF activity in healthy tissue, causing side-effects and even the formation of new tumors. Here we show the development of $BRAF^{V600E}$ kinase inhibitors of which the activity can be switched on and off reversibly with light, offering the possibility to overcome problems of systemic drug activity by selectively activating the drug at the desired site of action. Based on a known inhibitor, eight photoswitchable effectors containing an azobenzene photoswitch were designed, synthesized and evaluated. The most promising inhibitor showed an approximately 10-fold increase in activity upon light-activation. This research offers inspiration for the development of therapies for metastatic melanoma in which tumor tissue is treated with an active $BRAF^{V600E}$ inhibitor with high spatial and temporal resolution, thus limiting the damage to other tissues.

Graphical abstract:

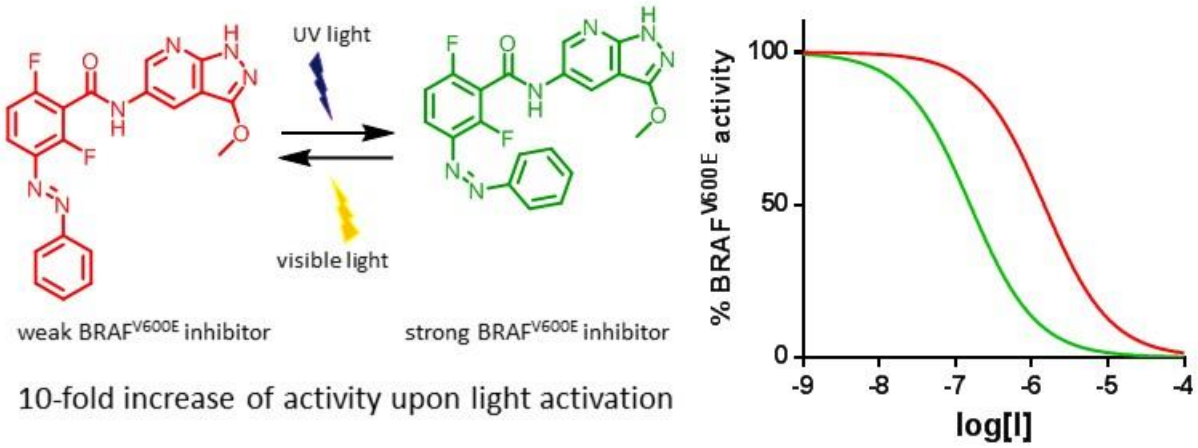

Introduction

Skin cancer is one the most frequently occurring types of cancer [1]. Of all skin cancers, melanoma has been reported to be the most deadly and challenging to treat [2]. Approximately 40 to 50% of melanomas harbor a mutation in the BRAF kinase [3], which is a cytosolic serine/threonine kinase belonging to the family of Rapidly Accelerated Fibrosarcoma (RAF) kinases. RAF kinases are part of the RAS/RAF/MEK/ERK signal transduction pathway which is involved in regulation of cell proliferation [4]. Increased activity of this pathway is often involved in the formation of cancer (**Fig. 1**). Due to the high frequency of the mutations and its role in the formation of cancer, the BRAF kinase became of clinical interest [3].

The activity of BRAF in cells is tightly regulated to prevent too extreme proliferation. Current hypothesis is that BRAF can be activated by dimerization and subsequent binding to RAS. While in the homo-dimeric state, it can also inactivate its binding partner through phosphorylation [5,6]. A single point mutation is believed to abolish the requirement of dimerization and binding to RAS for activation, resulting in elevated BRAF kinase activity in its monomeric form [7]. The most common BRAF mutation is V600E, which results in an about 500 times increased activity of the BRAF kinase compared to the wild-type [8]. Since a single mutation of the BRAF kinase drives the formation of a melanoma, $BRAF^{V600E}$ has become a therapeutic target. Currently two FDA-approved $BRAF^{V600E}$-selective ATP-competitive inhibitors are of use in the clinical practice. Vemurafenib (whose name is derived from **V**600**E mu**tated B**RAF in**h**ib**itor) has selectivity for $BRAF^{V600E}$ over $_{wt}$BRAF and is clinically used for the treatment of metastatic melanoma [9], alongside the second FDA approved $BRAF^{V600E}$ inhibitor, Dabrafenib (**Fig. 2.**) [10].

Unfortunately, $BRAF^{V600E}$ inhibitors Vemurafenib and Dabrafenib, used systemically, have several disadvantages. $BRAF^{V600E}$ inhibitors can increase the activity of the wild-type BRAF kinase in healthy cells, an effect known as “BRAF paradox” (See **Fig. 1**). This paradoxical activation is hypothesized to be caused by sub-saturated state of BRAF as a homo-dimer, in which the auto-inactivation mechanism is partially inhibited, resulting in a net increase of BRAF activity [10–12]. In healthy cells, increased activity of the RAS/RAF/MEK/ERK pathway promotes proliferation and development of new cancers, a fact that has been observed in some melanoma patients treated with $BRAF^{V600E}$ inhibitors [10,13]. The side effects observed with these kinase inhibitors illustrate that systemic exposure to chemotherapeutic agents can tremendously increase the disease burden. This highlights the importance of developing new concepts for spatial and temporal control over the exposure to, or activity of, chemotherapeutic agents.

The disadvantages of systemically used chemotherapeutic agents inspire, amongst others, the development of innovative solutions for local drug activation/inactivation by external control. Such approaches have the potential to improve the exposure of diseased tissue and to reduce the exposure of healthy tissue to active chemotherapeutic agents, whereas the disease tissue can be treated with higher doses. The emerging field of photopharmacology [14–17] offers a technology that enables local activation of chemotherapeutic agents by using light to control drug activity (see **Fig. 1**). Irreversible control can be acquired by the introduction of a photocleavable protecting group, which will result in a pro-drug that can be light-activated [18]. This has been successfully achieved for many chemotherapeutic agents[19], including $BRAF^{V600E}$ inhibitor Vemurafenib [20]. Reversible photocontrol over drug activity is being achieved through the introduction of a photoswitchable functional group, such as the frequently used azobenzene, into the structure of bioactive compounds. Azobenzene (See **Fig. 2**, highlighted in blue) is stable in the *trans* isomer and, upon irradiation with UV light, can be switched to the *cis* isomer [21]. This process can be reversed

thermally or *via* irradiation with visible light. The two photoisomers of azobenzene differ in structure, polarity and solubility [22] and these differences can be employed to design molecules with photoswitchable biological activity. Since isomerization from *trans* to *cis* can only be achieved photochemically, while re-isomerization from *cis* to *trans* occurs both photochemically and thermally, the fraction of *cis* isomer is more easily regulated. Therefore, it is preferred to carefully design molecules in which the *cis* isomer is more active than the *trans* isomer [15].

The photopharmacology approach has been successfully applied for molecules inspired by anti-cancer drugs such as Vorinostat [23], Bortezomib [24,25] and Combretastatin A4 [26–29]. Also for kinases, several photocontrolled inhibitors have been reported. For example, the group of Grøtli acquired control over the activity of the RET kinase [30], the group of Branda over the activity of Protein Kinase C [31] and the group of Peifer of the activity of vascular endothelial growth factor receptor 2 (VEGFR2) [32]. This sets the stage to apply this concept to develop molecules that enable reversible, spatial and temporal control over the activity of $BRAF^{V600E}$ using light. Yet, the development of kinase inhibitors with photocontrolled activity has been shown to be challenging [33]. This is supported by a review of Hüll *et al.*, which reports 123 photoswitchable bioactive compounds [17], with only three of them targeting a kinase [30–32], even though kinase inhibitors are of high clinical interest. More recently, the groups of Peifer and Herges reported photo-switchable kinase inhibitors for the p38α MAPK and CK1β kinases. For these photo-switchable kinase inhibitors, small differences in activity between photo-isomers was observed, probably due to conformational adaptation of the kinase to either one of the photo-isomers of the ligand and/or irreversible reduction of diazo as the key causes for small differences in activity between photo-isomers [34].

Here we describe the design, synthesis and evaluation of $BRAF^{V600E}$ inhibitors with photocontrolled activity, whose structure was inspired by an analog of Vemurafenib. In total, eight $BRAF^{V600E}$ inhibitors were synthesized and their photochemical properties were determined. Subsequently, the activities of both their respective *trans* and *cis* isomers were determined in a cell-free $BRAF^{V600E}$ Western-blot-based activity assay, followed by cell cytotoxicity studies and kinome off-target screening for the most promising inhibitor.

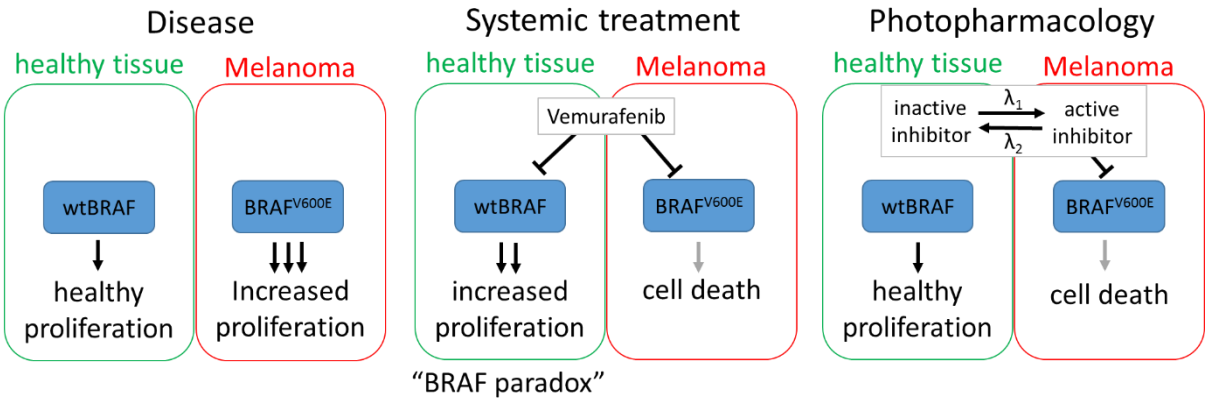

Fig. 1: *Conceptual description of the comparison between the disease (left), the systemic Vemurafenib treatment of Melanoma (middle) and the photopharmacological approach (right). Left: The* $BRAF^{V600E}$ *mutation drives the cell proliferation, resulting in cancer. Middle: For the treatment of Melanoma, Vemurafenib is active in both healthy and cancerous tissue, where in healthy tissue it can paradoxically increase the activity of the downstream pathway resulting in increased proliferation and potentially in the formation of new tumors. In melanoma, Vemurafenib induces cell death. Right: The photopharmacological approach aims to use an inactive inhibitor in healthy tissue that does not affect proliferation, while in melanoma the* $BRAF^{V600E}$ *inhibitor can be locally switched on with light, inducing cell death.*

Results and discussion

Numerous inhibitors for the $BRAF^{V600E}$ kinase, including the FDA-approved drugs Vemurafenib and Dabrafenib, harbor a common motif (**Fig. 2**, red), which consists of a benzene ring with a sulfonamide and a fluorine substituents. Group X on the sulfonamide is generally a propyl or aryl group, while the Y group is usually hydrogen or fluorine and the Z group consists of heterocycles, coupled either directly (such as in Dabrafenib) or by a carbonyl linker (such as in Vemurafenib) on an amide [35–40]. As demonstrated by co-crystal structures of $BRAF^{V600E}$ bound to its inhibitors [36–39], the common motif and the Z group are flat or under a small angle in the ATP binding pocket, where the heterocycles of the Z group form hydrogen bonds with Cys532. In contrast to the rest of the inhibitor, which is planar, the sulfonamide is bent, resulting in an approximate 90 degrees angle between the common motif and the X group. This X group binds in a small pocket, stabilized by interactions between the sulfonamide and Gly596, Phe595 and Asp594.

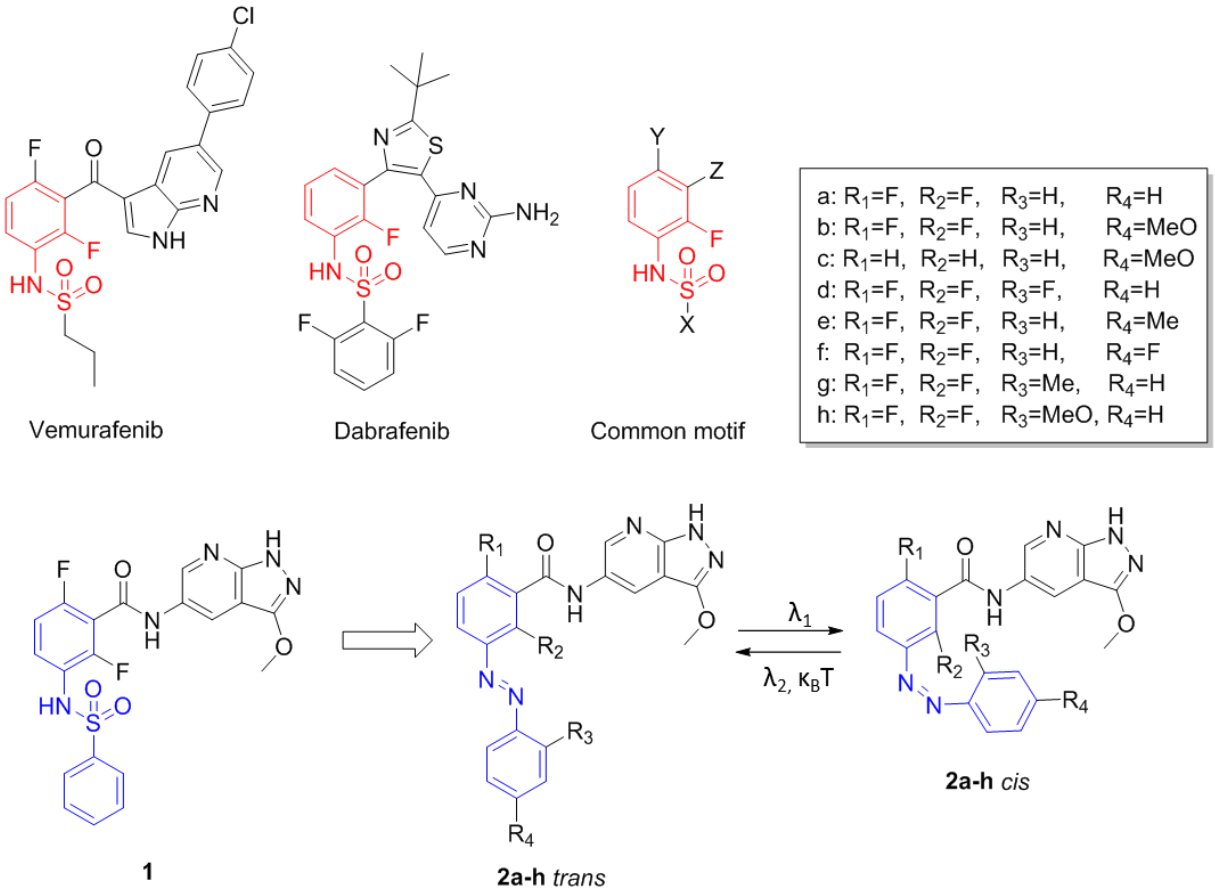

***Fig. 2**: Top: structure of Vemurafenib, Dabrafenib and a common motif found in many BRAF^{V600E} inhibitors. Bottom: Compound **1** has been reported as an improved Vemurafenib analog. Inspired by compound **1**, eight photoswitchable BRAF^{V600E} inhibitors **2a-h** were designed. Upon irradiation with light of wavelength λ_1, trans-**2a-h** can be switched to cis-**2a-h** cis. This isomerization can be reversed by irradiation with light of wavelength λ_2 or in a thermal relaxation process.*

A straightforward choice for the design of a photoswitchable BRAF^{V600E} inhibitor would be the replacement of the sulfonamide of Dabrafenib by a diazo group, introducing a photoswitchable azobenzene, along the principles of azologization [41]. However, Dabrafenib itself is already photochemically unstable. Upon UV light irradiation, a side-product is irreversibly formed, which is biologically less active [42]. This process might compete with

photoisomerization, which makes Dabrafenib unsuitable as a starting point for a photoswitchable inhibitor. Our design of a photoswitchable $BRAF^{V600E}$ inhibitor was instead based on compound **1** (**Fig. 2**), which was found upon optimization of Vemurafenib [43]. We selected compound **1** as a starting point to design photoswitchable analogs. This compound contains three aromatic moieties coupled by either an amide or a sulfonamide linker. Both linkers provides a site for replacement by a diazo group to generate inhibitors with an azobenzene photoswitch. Yet, when comparing into the binding mode of inhibitors in co-crystals with the $BRAF^{V600E}$ mutant, it became apparent to us that the two aromatic rings coupled by the amide are in one plane or deviate only slightly from this plane. Replacement of this amide by a *trans* isomer of the azobenzene functionality would provide inhibitors that retain the orientation of these rings. In crystal structures, the two aromatic rings coupled by the sulfonamide adopt a bent conformation. Therefore we anticipate that replacement of the sulfonamide by the *cis* isomer of the azobenzene functionality would retain the bio-active conformation. Since the concept of photo-activation requires activity of the *cis* isomer and inactivity of the *trans* isomer (*vide supra*), we chose to replace the sulfonamide functionality of **1** by a diazo group. We note, however, that the sulfonamide is involved in binding to the $BRAF^{V600E}$ kinase and we, therefore, anticipated a decrease of activity.

For bio-active compounds with photocontrolled activity, every chemical modification to the structure potentially changes both the biological and photochemical properties such as the position of the absorption band, the rate of thermal relaxation of the *cis* isomer back to the *trans* isomer and the highest ratio between *trans* and *cis* that can be achieved upon irradiation at photo-stationary state (PSS). Optimizing photocontrolled inhibitors with respect to all the parameters proved to be challenging, because a maximal difference in biological activity between both photo-isomers had to be achieved, while retaining optimal *trans*-*cis* ratios at PSS and half-life of the *cis* isomer. First, compound **2a** was designed to determine the effect of replacing the sulfonamide group with a diazo linker. While the percentages of the *cis* isomer at PSS of unsubstituted azobenzenes are usually relatively low, installing a *p*-

MeO group enable improvement to more than 95% of the *cis* isomer upon isomerization [44]. This idea inspired the design of compound **2b** with a *p*-MeO on the azobenzene photoswitch. The MeO group was moved to the *ortho* position in compound **2h**, with the idea that this can also improve the ratio of isomers at PSS. Compound **2c** was designed to determine the effect of both the fluorine atoms at the R_1 and R_2 position. Compounds **2d and 2f** were inspired by the SAR described by Wenglowsky *et al*.,[43] where fluorine at R_3 increase the activity of the inhibitor, while at R_4 it showed opposite effects. To increase the steric bulk, compound **2e** and **2g** were designed with a methyl substituent at either the *ortho* or *para* position.

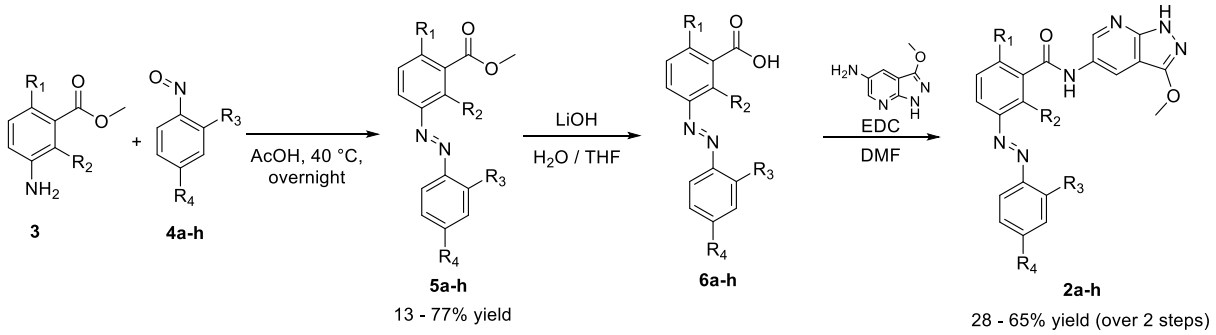

***Scheme 1**: Synthesis of BRAF^{V600E} inhibitors with photocontrolled activity*

Photoswitchable BRAF^{V600E} inhibitors **2a-h** were synthesized (**Scheme 1**) by condensing anilines **3** and nitrosobenzenes **4a-h** under standard Mills reaction conditions (see Supporting Information)**.** Subsequently, the methyl ester of **5a-h** was hydrolyzed using LiOH and the resulting acid was coupled to a previously reported [35] 3-methoxy-1H-pyrazolo[3,4-b]pyridine-5-amine, giving the final compounds **2a-h**. Thus we generated eight photoswitchable BRAF^{V600E} inhibitors.

Photochemical properties of compounds 2a-h

Next, the photochemical properties of these eight photoswitchable BRAF^{V600E} inhibitors were determined and the results are shown in **Table 1**. Compounds **2b** and **2c** containing a *p*-MeO substituent have absorption maxima in DMSO at λ = 357 nm and 352 nm, respectively. All other inhibitors have absorption maxima at λ's ranging from 332 to 340 nm. When

recording absorption spectra in the more biologically relevant BRAF assay buffer, the absorption bands show small hypsochromic shifts, yet all retain their maxima between 328 and 345 nm.

Using NMR spectroscopy, the distribution of isomers at the photo-stationairy state (PSS) upon irradiation with 365 nm light was determined, to quantify the efficiency of photochemical *trans-cis* isomerization. Unsubstituted compound **2a** can only reach 55% *cis* at PSS. Methoxy substituents at the R_3 and R_4 positions of **2b**, **2c** and **2h** resulted in near-quantitative switching. Methyl and fluorine substituents (compound **2d-g)** result in a PSS of between 61 and 84%.

To determine the rate of thermal *cis-trans* relaxation, the half-lives of the *cis* isomers were determined in both DMSO and the BRAF assay buffer at room temperature. In DMSO, for all compounds relatively long half-lives were observed. The half-life of the *cis* isomer of compounds **2a** and **2c** was determined in BRAF assay buffer to be shorter than in DMSO, yet the half-lives are still in the hour range. Of all other compounds, the half-lifes of the respective *cis* isomers were determined in a 1:1 mixture of BRAF assay buffer and acetonitrile, for solubility reasons. In this mixture, long half-lives of over a day were observed at room temperature. From the measured half-lives we concluded that the extend of thermal relaxation from *cis* to *trans* during the 1 h reaction time used in the western blot $BRAF^{V600E}$ activity assay (*vide infra*) is very limited.

Table 1: *Photochemical properties*

compound	structure	$\lambda_{max,trans}$ DMSO	$t_{1/2}$ *cis* At rt DMSO	% *cis* at PSS	$\lambda_{max,trans}$ BRAF assay buffer	$t_{1/2}$ *cis*[2]
2a	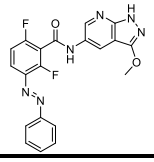	332 nm	> 10 h	55%	328 nm	5.4 h

2b	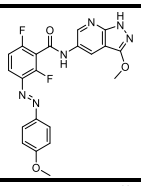	357 nm	> 10 h	92%	341 nm	> 24 h *
2c	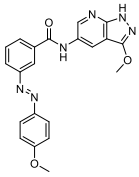	352 nm	> 10 h	94%	345 nm	> 10 h
2d	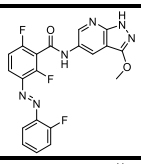	336 nm	> 20 h	71%	331 nm	~5 h *
2e	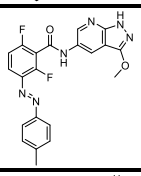	340 nm	> 20 h	84%	338 nm	> 24 h *
2f	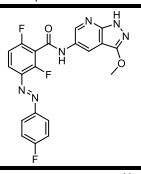	335 nm	> 20 h	62%	338 nm	> 24 h *
2g	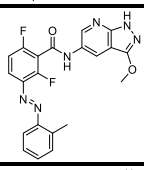	335 nm	> 70 h	77%	334 nm	> 24 h *
2h	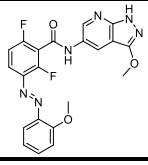	334 nm	> 24 h	88%	327 nm	> 24 h *

[1] in DMSO

[2] At room temperature in BRAF assay buffer * (50% ACN)

Biological evaluation

The activity of the $BRAF^{V600E}$ inhibitors was determined using an assay [45] with purified recombinant $BRAF^{V600E}$ with inactive MEK-1 as a substrate, and the enzymatic activity was determined by quantifying the phosphorylated-MEK-1 product using Western Blot. Prior to the assay, the inhibitor was either heated for 30 min at 60 °C to fully thermally adapt to the *trans* isomer or irradiated with 365 nm light for 45 min to reach PSS (see **Table 1**)

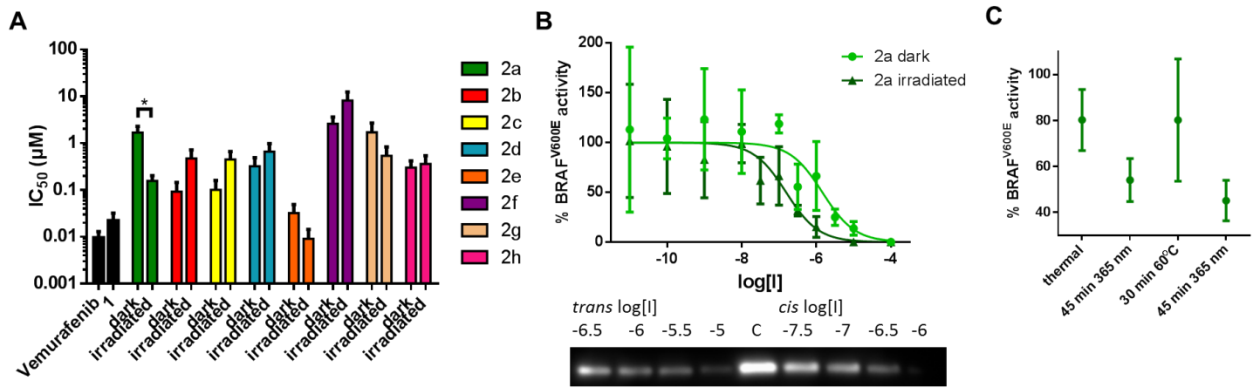

***Fig. 3**: BRAF^{V600E} activity assay. **A:** IC_{50} values as determined using the BRAF^{V600E} assay. **B:** Top: dose-response curve of **2a** in trans and cis. Bottom: Western Blot detection of p-MEK1. **C:** Kinase activity after sequential switching, by irradiation from trans to cis, thermal relaxation to trans and irradiation from trans to cis, at 1 μM of **2a** (N=2, ± S.D.)*

First, the IC_{50} values of the reference compounds Vemurafenib and compound **1** were determined to be 9.6 ± 3.3 nM and 22 ± 10 nM, respectively (**Fig. 3A**). Compound **2a**, with H as substituents at R_3 and R_4, showed an IC_{50} in the dark of 1.68 ± 0.62 μM, which decreased to 156 ± 47 nM upon light-induced switching to the *cis* isomer, resulting in an approximately 10-fold increase in activity upon irradiation, as shown in **Fig. 3B**. Furthermore, the reversibility of this activation was determined, as demonstrated in **Fig. 3C**: going through a cycle of switching to *cis* with UV light and thermal re-isomerization, the original activity was recovered, indicating that the irradiation leads to reversible isomerization of the azobenzene moiety and does not result in an irreversible photodegradation. We have observed that, as compared to **1**, compound **2a** lost some of the potency, likely due to the loss of the beneficial interactions of the sulfonamide within the active site. Unfortunately, the photochemical properties of compound **2a** are suboptimal, with only 55% of the active *cis* isomer at PSS.

Compared to compound **2a**, installing a para-alkyloxy substituent on azobenzenes usually results in near quantitative isomerization from *trans* to *cis*, as was also observed for compounds **2b** and **2c**, bearing a MeO substituent at the R_4 position. Even though **2b** and **2c** show improved photo-isomerization compared to **2a**, no statistically significant difference in

kinase inhibitory activity between the dark and irradiated state was observed for either compound. The difference between **2b** and **2c** is the presence of two fluorine substituents at the R_1 and R_2 position of compound **2b**. However, having the two fluorines replaced by hydrogen in compound **2c** did not affect the biological activity.

Additional fluorine substituents were placed at the R_3 position in compound **2d** and at the R_4 position of compound **2f**. Both for compound **2d** and **2f** no statistically significant difference in activity between the dark and irradiated state was observed and the fluorine substituents resulted in less active inhibitors. In contrast to placing a small fluorine substituent at the R_4 position – surprisingly – a methyl substituent on this position of compound **2e** resulted in improved activity. Even though no difference in activity between the dark and irradiated state of **2e** was observed, the inhibitor has an IC_{50} value comparable to reference compound **1** and Vemurafenib. Furthermore, the influence of *ortho* substituents was further determined with compound **2g** with a methyl at the R_3 position and compound **2h** with a methoxy substituent at the R_3 position, again showing no statistically significant difference between the dark and irradiated state a further loss of potency.

In the enzymatic assay, the activity of compound **2a** increased approximately 10-fold upon irradiation. To determine if the observed difference in activity from the enzyme assay could be translated to a difference in cytotoxicity, cell viability experiments were performed in A375 cells, a melanoma cell line - harboring the $BRAF^{V600E}$ mutation – which is commonly used to study the cytotoxicity of $BRAF^{V600E}$ inhibitors [12,38,40,46]. However, upon incubation for 24h (see **Fig. 4a**), no cytotoxicity was observed for both **2a** in the dark and irradiated state, where both reference compounds resulted in lower cell viability. The inhibition of $BRAF^{V600E}$ by compound **2a** in the enzymatic inhibition assay could not be translated to cytotoxicity in A375 cells, possibly due to off-target activity for other kinases or escape routes to the RAS/RAF/MEK/ERK proliferation pathway.

In the development of kinase inhibitors, it has proven to be very challenging to develop inhibitors with high selectivity towards other kinases [47]. This implies that azologization of a

selective kinase inhibitor can potentially result in a loss of selectivity among kinase isoenzymes. To acquire a deeper understanding of other effects of the photoswitchable $BRAF^{V600E}$ kinase inhibitor **2a**, the kinome inhibition profile was investigated using Pamgene STK Chips, which is a well-established method for target evaluation [48,49]. Cell lysates from SK-Mel-28 cell were treated with DMSO as a control, compound **1** on which the photoswitchable inhibitors were based and compound **2a** (both dark and irradiated) (See **Fig. 4B)**. Compared to the DMSO control, compound **1** resulted in a decrease in kinase activity in the cell lysates. Interestingly, treatment with compound **2a** (dark) resulted in a general increase in phosphorylation activity (See. **Fig. 4C**). In line with the expectation, treatment of **2a** (irradiated) showed a decrease in phosphorylation activity compared to the **2a** (dark), which corresponds to increased kinase inhibition upon irradiation. However, compared to the DMSO control, the general phosphorylation level upon **2a** (irradiated) treatment is still elevated. This could be explained by the presence of **2a** *trans* in the irradiated state, where irradiation with λ = 365 nm light results in only 55% of the more active *cis* isomer. Yet, the unexpected increased phosphorylation level in lysates SK-MEL28 observed for compound **2a** in both the dark and irradiated state fit with the lack of cytotoxicity of compound **2a** in A375 cells.

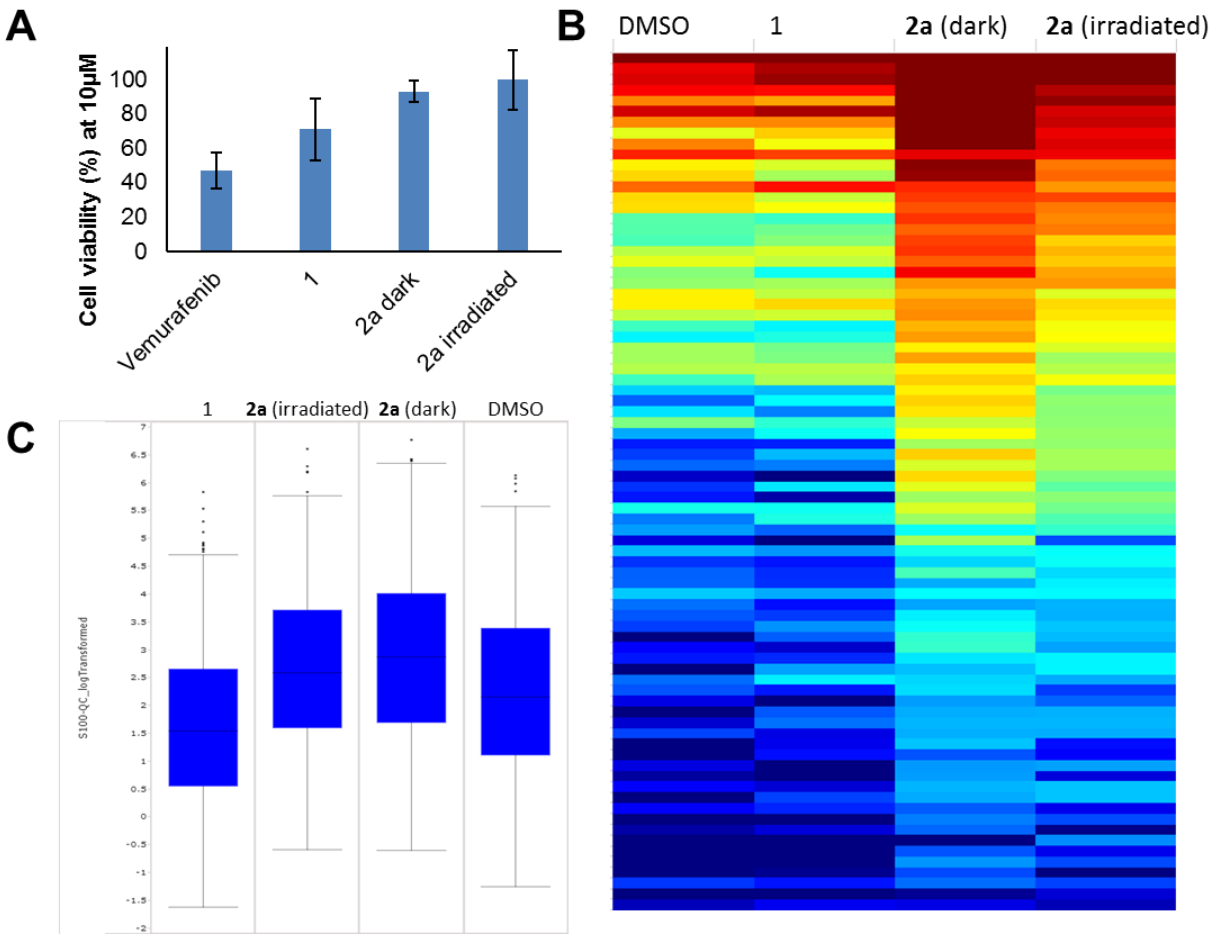

Fig. 4: ***A****: Cell viability MTS assay of A375 cells after 24 h incubation with 10µM Vemurafenib, compound* ***1****, compound* ***2a*** *thermally adapted and irradiated, all compared to DMSO.* ***B-C****: Kinome profiling using cell lysates from SK-Mel-28 cells. The lysates were treated with a DMSO control, reference compound* ***1****, compound* ***2a*** *dark and compound* ***2a*** *irradiated with 365 nm light (in vitro inhibition).* ***B****: Heatmap showing log2-transformed signal intensities of the phosphorylated peptides included on the STK arrays. The signals were sorted from high (red) to low (blue) intensity.* ***C****: Box plots summarizing the overall peptide phosphorylation levels depicted in C.*

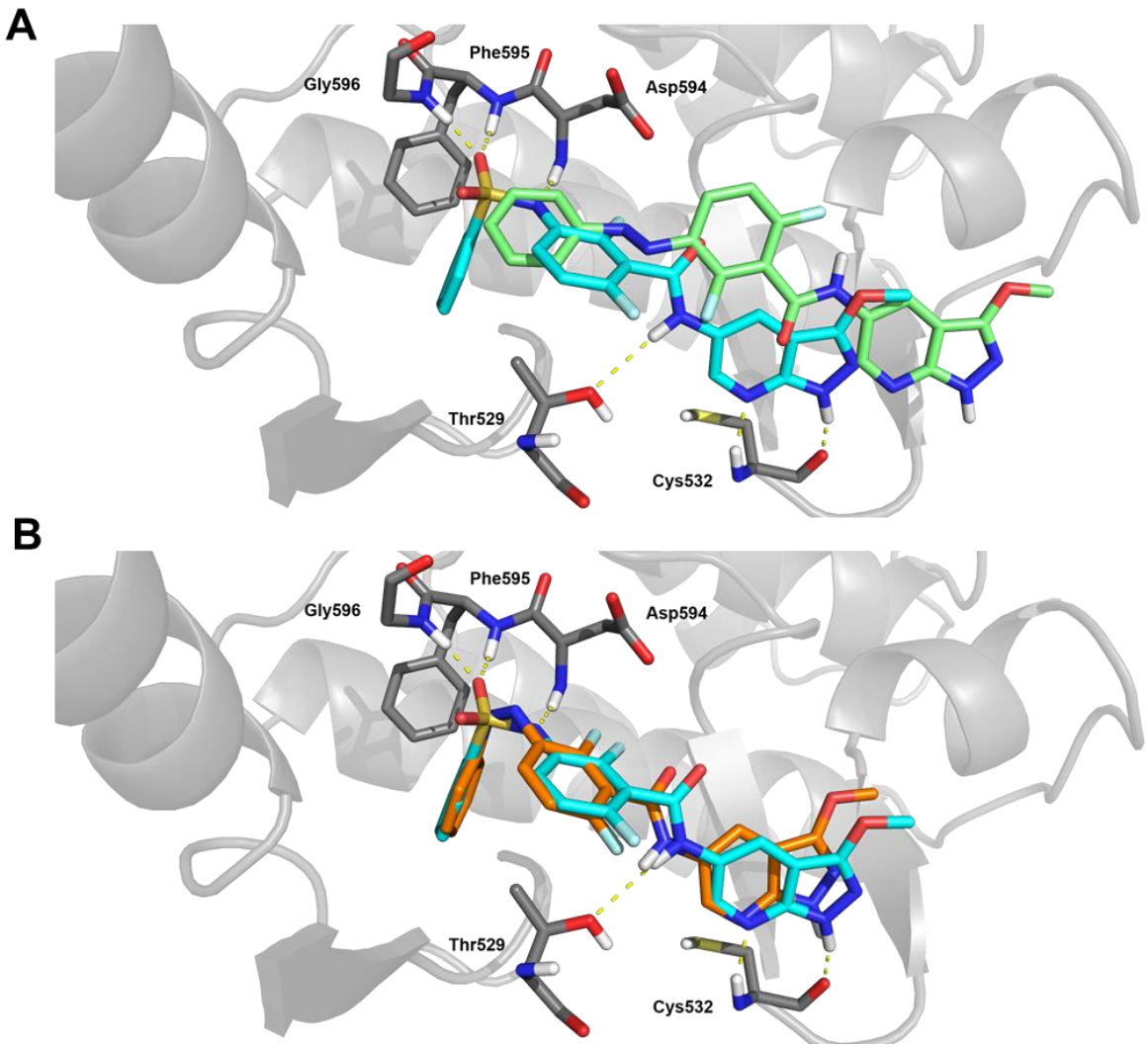

Fig. 5*: Binding site of BRAF^{V600E} cocrystallized with compound **1** (PDB ID: 3SKC, protein in grey and ligand in cyan), superimposed on the docking poses of (**A**) compound **2a** trans (green) and (**B**) compound **2a** cis (orange). Hydrogen bonds are depicted as yellow dashed lines.*

As an important prerequisite for any future in vivo applications, we have further tested the plasma stability of compound **2a**. First, photo-isomerization of compound **2a** in bovine plasma was studied (see Fig. S7.1). Irradiation with 365 nm results in a decrease of the absorption band of **2a** *trans*, however, surprisingly, irradiation with white light does not result in photo-isomerization back to the trans isomer. The same photochemical behavior is observed after incubation of 1h at 37 ^{o}C prior to photo-isomerization (see Fig S7.2), which suggests at least partial preservation of the azobenzene fragment. When compound **2a** was

pre-irradiated with 365 nm light in DMSO, added to plasma and incubated at 37 ^{o}C for 1 h, reversible photo-isomerization was observed (See Fig. S7.3). Finally, compound **2a** was incubated for 20 h in bovine plasma at 37 ^{o}C, after which by LCMS masses of both isomers (See Fig S.7.4 to S7.7) of the fully intact molecules were detected. An additional peak corresponding to an unknown product was observed, of which the mass doesn't match with products of azobenzene reduction. Altogether, this further supports that 20h of plasma incubation does not fully degrade photoswitchable $BRAF^{V600E}$ inhibitor **2a**

Finally, to rationalize the 10-fold difference in BRAF inhibitory potency between the two isomers of inhibitor **2a**, both photo-isomers were docked into the crystal structure of $BRAF^{V600E}$. As shown in **Fig. 5A**, compound *cis*-**2a** shows a nearly perfect overlap with reference compound **1**. However, due to the replacing the sulfonamide for a diazo bridge, the interactions with the Asp594, Phe595 and Gly596 backbone are no longer present, which could explain the drop in potency of compound **2a** compared to compound **1**. Still, *cis*-**2a** and **1** are spectacularly close in conformation, demonstrating that *cis*-azobenzenes are suitable for mimicking diarylsulfonamide moieties in drugs. Also *trans*-**2a** was docked into the same crystal structure, as shown in **Fig. 5B**. Compound *trans*-**2a** docked into a conformation that is completely different from the original compound **1**, thus indicating binding of this isomer to the kinase active site is perturbed. The docking data of **2a** trans suggest that bulky groups at the R_1 position might disfavor binding of the *trans* isomer and decrease the activity, which could potentially improve the difference in activity between *trans* and *cis* of **2a**.

Discussion

In the emerging field of photopharmacology, the development of kinase inhibitors has been very challenging and only a few examples have been reported [30–32]. Herein, we show a proof of concept for the development of a $BRAF^{V600E}$ inhibitor with photocontrolled activity, which is a reversibly photocontrolled inhibitor for a therapeutically relevant kinase. We have identified compound **2a**, which has a difference in activity between the thermal and irradiated state of 10-fold, even though a PSS of only a 55% *cis* was achieved upon irradiation. Using docking studies, we rationalized the binding of both *cis* and *trans*, which indicates how photo-isomerization can change activity. Using kinome screening, it was found that azologization of compound **1** to provide compound **2a** resulted in increased kinase activity for both dark and irradiated samples, which could explain the observed lack of cytotoxicity for the $BRAF^{V600E}$ inhibitor photo-isomers in A375 cells, despite their 10-fold difference in activity in the ATP-competitive enzyme inhibition studies. This demonstrates the importance of off-target screening in the development of photoswitchable kinase inhibitors.

Selective $BRAF^{V600E}$ inhibitors with light-controlled activity will provide opportunities for local and precise treatment of $BRAF^{V600E}$-driven tumors, without harming the activity of the RAS/RAF/MEK/ERK pathway in healthy cells and tissues. Selective UV light irradiation of $BRAF^{V600E}$-driven tumors activates the inhibitor and can besides that possibly be of additional therapeutic value by inducing phototoxicity. Indeed, UV light irradiation is used for treating other types of skin cancer such as Cutaneous T-Cell lymphoma in which irradiation results in apoptosis [50]. Furthermore, in a research setting, a $BRAF^{V600E}$ inhibitor with light-controlled activity will be a powerful research tool [51] to study the kinase and its interplay with other proteins that control the activity of the RAS/RAF/MEK/ERK pathway. Photocontrolled inhibitors allow for short-term BRAF activation and inactivation in a fully reversible manner. Besides that, spatial control allows for local modulation of BRAF activity with high resolution. Such insights are particularly relevant for the BRAF kinase because of the complex mechanisms involved in its regulation, which will contribute to develop better therapies for melanoma in the future.

Acknowledgements

The support of the Netherlands Organization for Scientific Research (NWO-CW VIDI grants 723.014.001 to W.S. and 723.012.005 to F.D.) is kindly acknowledged. We would like to thank Konstantin Hoffer (UCCH Kinomics Hamburg) for technical support and acknowledge SFB 677 “Function by Switching” (Collaborative Research Center financial Support by DFG) for financial support.

Synthetic procedures.

3: Methyl 2,6-difluoro-3-(phenyldiazenyl)benzoate.

A solution of methyl 3-amino-2,6-difluorobenzoate (6.60 mmol, 1.23 g, Combi-Blocks) and nitrosobenzene (6.00 mmol, 642 mg) in acetic acid (30 mL) was heated at 40 °C overnight. Afterwards, the reaction mixture was diluted with diethyl ether (200 mL) and washed with 1N aq. HCl (2 x 150 mL), sat. aq. $NaHCO_3$ (150 mL) and brine (150 mL). The organic phase was dried ($MgSO_4$) and filtered through a plug of silica. The volatiles were removed *in vacuo* and to the residue was added hot pentane (200 mL). The resulting suspension was filtered and the volatiles were removed to provide product as red powder (1.27 g, 77%). R_f = 0.50 (pentane/Et_2O, 1:1, v/v); Mp. 78-79 °C; ^{1}H NMR (400 MHz, $CDCl_3$): δ 4.02 (s, 3H), 7.01-7.06 (m, 1H), 7.50-7.55 (m, 3H), 7.90-7.96 (m, 3H); ^{13}C NMR (100 MHz, $CDCl_3$): δ 53.0, 112.2 (dd, J_{C-F} = 4.2 Hz, J_{C-F} = 23.2 Hz), 120.8 (dd, J_{C-F} = 2.0 Hz, J_{C-F} = 10.7 Hz), 123.2, 129.2, 131.8, 137.5 (dd, J_{C-F} = 4.1 Hz, J_{C-F} = 6.3 Hz), 152.2, 160.0 (dd, J_{C-F} = 6.5 Hz, J_{C-F} = 268 Hz), 161.5, 161.8 (dd, J_{C-F} = 5.7 Hz, J_{C-F} = 262 Hz); ^{19}F NMR (376 MHz, $CDCl_3$): -120.5 (m), -105.9 (m); HRMS (ESI+) calc. for $[M+H]^+$ ($C_{14}H_{11}F_2N_2O_2$): 277.0783, found: 277.0783.

4: 2,6-difluoro-3-(phenyldiazenyl)benzoic acid.

To a solution of compound **3** (1.80 mmol, 500 mg) in THF (15 mL) was added sat. aq. LiOH (10 mL). The resulting biphasic mixture was vigorously stirred for 5h, after which the volatiles were evaporated. 1N aq. HCl (30 mL) was added to the residue, the resulting precipitate was filtered off and redissolved in AcOEt (60 mL). The solution was dried ($MgSO_4$) and the volume was reduced. The product was precipitated by addition of pentane, filtered off and washed with pentane to give orange solid (186 mg, 40%). Mp. 175-176 °C; ^{1}H NMR (400 MHz, DMSO-d_6): δ 7.36 (t, ^3J = 8.8 Hz, 1H), 7.56-7.65 (m, 3H), 7.85-7.94 (m, 3H); ^{13}C NMR (100 MHz, DMSO-d_6): δ 113.4 (dd, J_{C-F} = 3.8 Hz, J_{C-F} = 23.4 Hz), 114.0 (dd, J_{C-F} = 20.3 Hz, J_{C-F} = 21.1 Hz), 120.8 (d, J_{C-F} = 10.9 Hz), 123.3, 130.0, 132.7, 137.3 (dd, J_{C-F} = 3.9 Hz, J_{C-F} =

7.2 Hz), 152.3, 157.1 (dd, J_{C-F} = 7.6 Hz, J_{C-F} = 264 Hz), 161.2 (dd, J_{C-F} = 6.7 Hz, J_{C-F} = 258 Hz), 162.0; ^{19}F NMR (376 MHz, DMSO-d_6): -123.0 (m), -107.1 (m); HRMS (ESI+) calc. for $[M+H]^+$ ($C_{13}H_9F_2N_2O_2$): 263.0627, found: 263.0625.

***Trans*-2a: 2,6-difluoro-*N*-(3-methoxy-1H-pyrazolo[3,4-b]pyridin-5-yl)-3-phenyldiazenyl)-benzamide.**

A solution of compound **4** (0.38 mmol, 100 mg), 3-methoxy-1H-pyrazolo[3,4-b]pyridin-5-amine (0.37 mmol, 60 mg, prepared by a published procedure [52]) and EDC (0.42 mmol, 80 mg) in DMF (5 mL) was stirred at rt overnight. Afterwards, the reaction mixture was diluted with ethyl acetate (80 mL) and washed with brine (2 x 60 mL) ,1N aq. HCl (2 x 60 mL), sat. aq. $NaHCO_3$ (60 mL) and again brine (60 mL). The organic phase was dried ($MgSO_4$). The volatiles were partially removed *in vacuo* and to the residue was added pentane (200 mL). The resulting precipitate was filtered to provide product as orange powder (65 mg, 43%). R_f = 0.62 (pentane/AcOEt, 1:1, v/v); Mp. >250 °C; ^{1}H NMR (400 MHz, DMSO-d_6): δ 4.01 (s, 3H), 7.44 (t, ^3J = 8.8 Hz, 1H, Ar**H**), 7.55-7.66 (m, 3H), 7.85-7.97 (m, 3H), 8.52 (d, ^4J = 2.0 Hz, 1H), 8.61 (d, ^4J = 2.0 Hz, 1H), 11.22 (s, 1H), 12.61 (s, 1H); ^{13}C NMR (100 MHz, DMSO-d_6): δ 56.1, 102.9, 113.4 (dd, J_{C-F} = 3.5 Hz, J_{C-F} = 23.3 Hz), 116.7 (dd, J_{C-F} = 21.0 Hz, J_{C-F} = 23.6 Hz), 119.0, 120.4 (d, J_{C-F} = 10.7 Hz), 123.3, 128.4, 130.1, 132.8, 137.3 (dd, J_{C-F} = 3.8 Hz, J_{C-F} = 7.2 Hz), 143.9, 150.1, 152.4, 155.1, 156.6 (dd, J_{C-F} = 8.1 Hz, J_{C-F} = 260.4 Hz), 158.1, 160.8 (dd, J_{C-F} = 7.1 Hz, J_{C-F} = 254.8 Hz); ^{19}F NMR (376 MHz, DMSO-d_6): -124.0 (m), -108.6 (m); HRMS (ESI+) calc. for $[M+H]^+$ ($C_{20}H_{15}F_2N_6O_2$): 409.1219, found: 409.1211.

***Cis*-2a:**

A solution of compound ***trans*-2a** in DMSO-d_6 (0.5 mL, ~2 mg/mL) was irradiated at λ = 365 nm (distance ~1 cm) to provide a sample of 55% ***cis*-2a**. ^{1}H NMR (400 MHz, DMSO-d_6): δ 3.99 (s, 3H), 6.94 (d, ^3J = 8.0 Hz, 2H), 7.08-7.14 (m, 1H), 7.18-7.32 (m, 2H), 7.39 (app t, ^3J = 8.0 Hz, 2H), 8.42 (d, ^4J = 2.4 Hz, 1H), 8.54 (d, ^4J = 2.0 Hz, 1H), 11.05 (s, 1H), 12.58 (s, 1H); ^{19}F NMR (376 MHz, DMSO-d_6): -122.4 (m), -114.1 (m).

5: Methyl 2,6-difluoro-3-((4-hydroxyphenyl)diazenyl)benzoate.

Methyl 3-amino-2,6-difluorobenzoate (2.00 mmol, 374 mg) was dissolved in 1N aq. HCl (5.0 mL) and the solution was cooled in an ice-water bath. A solution of $NaNO_2$ (2.50 mmol, 173 mg) in water (1.0 mL) was added, and the reaction mixture was stirred for 10 min. A solution of phenol (1.80 mmol, 169 mg) and KOH (3.60 mmol, 202 mg) in MeOH (2.5 mL) was added dropwise and the cooling was removed. After 10 min stirring, the reaction mixture was diluted with AcOEt (80 mL) and washed with 1H HCl (2 x 60 mL) and brine (80 mL). The organic phase was dried ($MgSO_4$) and the solvent was evaporated. The product was purified by flash chromatography (Silicagel, 40-63 μm, pentane:Et_2O, 9:1 to 1:1, v/v) to give orange powder (123 mg, 23%). R_f = 0.60 (pentane/Et_2O, 1:1, v/v). Compound **5** was used in the following step without further characterization.

6: Methyl 2,6-difluoro-3-((4-methoxyphenyl)diazenyl)benzoate.

To a solution of compound **5** (0.34 mmol, 100 mg) and methyl iodide (1.50 mmol, 94 μL) in acetone (5 mL) was added potassium carbonate (0.50 mmol, 69 mg). The resulting suspension was stirred at rt overnight, after which it was diluted with Et_2O (50 mL) wand washed with 1H HCl (2 x 40 mL), sat. aq. $NaHCO_3$ (2 x 40 mL) and brine (40 mL). The organic phase was dried ($MgSO_4$) and the solvent was evaporated. The product was purified by flash chromatography (Silicagel, 40-63 μm, pentane:Et_2O, 9:1, v/v) to give orange powder (100 mg, 96%). R_f = 0.64 (pentane/Et_2O, 7:3, v/v); Mp. 60-62 °C; ^{1}H NMR (400 MHz, $CDCl_3$): δ 3.88 (s, 3H), 4.02 (s, 3H), 6.95-7.05 (m, 3H), 7.84-7.92 (m, 1H), 7.91 (d, ^3J = 9.2 Hz, 2H); ^{13}C NMR (100 MHz, $CDCl_3$): δ 53.0, 55.6, 112.1 (dd, J_{C-F} = 4.1 Hz, J_{C-F} = 23.1 Hz), 114.3, 120.8 (dd, J_{C-F} = 2.3 Hz, J_{C-F} = 10.5 Hz), 125.3, 129.4, 137.7 (dd, J_{C-F} = 4.1 Hz, J_{C-F} = 7.3 Hz), 147.0, 157.8 (dd, J_{C-F} = 6.4 Hz, J_{C-F} = 267 Hz), 161.3 (dd, J_{C-F} = 5.7 Hz, J_{C-F} = 261 Hz), 161.6, 162.7; ^{19}F NMR (376 MHz, $CDCl_3$): -121.2 (m), -107.2 (m); HRMS (ESI+) calc. for $[M+H]^+$ ($C_{15}H_{13}F_2N_2O_3$): 307.0888, found: 307.0885.

7: 2,6-difluoro-3-((4-methoxyphenyl)diazenyl)benzoic acid.

To a solution of compound **6** (0.36 mmol, 110 mg) in THF (3 mL) was added sat. aq. LiOH (2 mL). The resulting biphasic mixture was vigorously stirred for 5h, after which the volatiles were evaporated. 1N aq. HCl (30 mL) was added to the residue, the resulting precipitate was filtered off and redissolved in AcOEt (60 mL). The solution was dried ($MgSO_4$) and the volume was reduced. The product was precipitated by addition of pentane, filtered off and washed with pentane to give compound **7** (51 mg, 48%). Compound **7** was used in the following step without further characterization.

***Trans*-2b: 2,6-difluoro-N-(3-methoxy-1H-pyrazolo[3,4-b]pyridin-5-yl)-3-((4-methoxyphenyl)-diazenyl)benzamide.**

A solution of compound **7** (0.116 mmol, 34 mg), 3-methoxy-1H-pyrazolo[3,4-b]pyridin-5-amine (0.15 mmol, 25 mg, prepared by a published procedure [52]) and EDC (0.16 mmol, 31 mg) in DMF (2 mL) was stirred at rt overnight. Afterwards, the reaction mixture was diluted with ethyl acetate (50 mL) and washed with brine (2 x 40 mL), 1N aq. HCl (2 x 40 mL), sat. aq. $NaHCO_3$ (40 mL) and again brine (40 mL). The organic phase was dried ($MgSO_4$). The volatiles were partially removed *in vacuo* and to the residue was added pentane (50 mL). The resulting precipitate was filtered to provide product as orange powder (14 mg, 28%). R_f = 0.72 (pentane/AcOEt, 1:1, v/v); Mp. = 248-250 °C; ^{1}H NMR (400 MHz, DMSO-d_6): δ 3.97 (s, 3H), 4.01 (s, 3H), 7.15 (d, ^3J = 8.8 Hz, 2H), 7.41 (t, ^3J = 8.8 Hz, 1H), 7.85-7.95 (m, 3H), 8.51 (d, ^4J = 2.0 Hz, 1H), 8.61 (d, ^4J = 2.0 Hz, 1H), 11.19 (s, 1H), 12.60 (s, 1H); ^{13}C NMR (100 MHz, DMSO-d_6): δ 56.1, 56.2, 102.9, 113.3 (dd, J_{C-F} = 3.7 Hz, J_{C-F} = 23.0 Hz), 115.3, 116.6 (dd, J_{C-F} = 21.1 Hz, J_{C-F} = 23.6 Hz), 118.9, 120.2 (d, J_{C-F} = 10.3 Hz), 125.5, 128.4, 137.4 (dd, J_{C-F} = 3.8 Hz, J_{C-F} = 7.3 Hz), 143.8, 146.8, 150.1, 155.1, 156.1 (dd, J_{C-F} = 8.0 Hz, J_{C-F} = 258.3 Hz), 158.2, 160.2 (dd, J_{C-F} = 7.1 Hz, J_{C-F} = 254.0 Hz), 163.2; ^{19}F NMR (376 MHz,

DMSO-d_6): -124.6 (m), -109.9 (m); HRMS (ESI+) calc. for $[M+H]^+$ ($C_{21}H_{17}F_2N_6O_3$): 439.1325, found: 439.1318.

***Cis*-2b:**

A solution of compound ***trans*-2b** in DMSO-d_6 (0.5 mL, ~2 mg/mL) was irradiated at λ = 365 nm (distance ~1 cm) to provide a sample of 92% ***cis*-2b**. ^{1}H NMR (400 MHz, DMSO-d_6): δ 3.75 (s, 3H), 3.99 (s, 3H), 6.94 (d, ^3J = 8.8 Hz, 2H), 7.02 (d, ^3J = 8.8 Hz, 2H), 7.12-7.18 (m, 1H) 7.27 (t, ^3J = 8.8 Hz, 1H), 8.42 (d, ^4J = 2.0 Hz, 1H), 8.54 (d, ^4J = 2.0 Hz, 1H), 11.04 (s, 1H), 12.58 (s, 1H); ^{19}F NMR (376 MHz, DMSO-d_6): -123.1 (m), -114.8 (m).

8: Ethyl (*E*)-3-((4-hydroxyphenyl)diazenyl)benzoate.

Ethyl 3-aminobenzoate (3.0 mL, 2.7 g, 17 mmol) was dissolved in aq. 1N HCl (50 mL) and $NaNO_2$ (1.60 g, 23 mmol) was added. The reaction mixture was stirred at 0^{o}C for 10 min. MeOH (25 mL) was added to the reaction mixture and a solution of PhOH (1.93 g, 14.6 mmol) and KOH (2.14 g, 38.1 mmol) in MeOH (20 mL) was added dropwise. The reaction mixture was stirred at room temperature for 1h. After completion, aq. 1N HCl (50 mL) and EtOAc (50 mL) were added to the reaction mixture and the water layer was extracted with EtOAc (3 x 50 mL). The combined organic layers were concentrated *in vacuo*, Et_2O was added (100 mL) and the product was filtered off and washed with pentane. The product was obtained as an orange solid (1.58 g, 5.8 mmol, 34% yield). Mp: 141-146 ^{o}C. ^{1}H NMR (400 MHz, $CDCl_3$) δ 1.44 (t, *J* = 7.1 Hz, 3H), 4.38 – 4.48 (m, 2H), 5.65 (s, 1H), 6.98 (d, *J* = 6.9 Hz, 2H), 7.58 (t, *J* = 7.8 Hz, 1H), 7.91 (d, *J* = 6.9 Hz, 2H), 8.05 (d, *J* = 7.9 Hz, 1H), 8.12 (d, *J* = 7.7 Hz, 1H), 8.52 (s, 1H). Compound **8** was used in the following step without further characterization.

9: Ethyl (*E*)-3-((4-methoxyphenyl)diazenyl)benzoate.

Compound **8** (0.70 g, 2.6 mmol) was dissolved in acetone (20 mL) and MeI (3.0 mL, 1.3 g, 9.3 mmol) and K_2CO_3 (3.7 g, 26.8 mmol) were added. The reaction mixture was stirred at 40

^{o}C overnight. After completion, Et_2O (50 mL) and water (50 mL) were added and the organic layer was separated, dried with $MgSO_4$ and concentrated *in vacuo*. The product was purified by flash chromatography (Silicagel 40 – 63 nm, pentane; 0-10% EtOAc in pentane). The product was obtained as an orange solid (0.62 g, 2.2 mmol, 85% yield). Mp: 40 - 42 ^{o}C. ^{1}H NMR (400 MHz, $CDCl_3$) δ 1.42 (d, *J* = 14.3 Hz, 3H), 3.85 (s, 3H), 4.42 (q, *J* = 7.1 Hz, 2H), 6.99 (d, *J* = 9.0 Hz, 2H), 7.54 (t, *J* = 7.8 Hz, 1H), 7.94 (d, *J* = 9.0 Hz, 2H), 8.11 (d, *J* = 7.9 Hz, 1H), 8.53 (s, 1H). ^{13}C NMR (101 MHz, $CDCl_3$) δ 14.4, 55.5, 61.2, 76.8, 77.1, 77.4, 114.2, 123.9, 125.0, 126.3, 129.0, 131.0, 131.6, 146.8, 152.7, 162.4, 166.1. HRMS (ESI+) calc. for. [M+H^{+}] ($C_{16}H_{17}N_2O_3$): 285.1234, found: 285.1232.

10: 3-((4-methoxyphenyl)diazenyl)benzoic acid.

Compound **9** (3.52 mmol, 1.00 g) was dissolved in a mixture of methanol (40 mL) and tetrahyrofuran (40 mL). Aqueous sodium hydroxide (2N, 20 mL) was added and the mixture was heated under reflux for 3 hours. The volatiles were evaporated, the residue was dissolved in aqueous HCl (1N, 20 mL) and extracted with ethyl acetate (2 x 20 mL). Organic phases were collected, dried and the product was purified by precipitation from AcOEt/pentane. Yield: 66%; orange powder. Mp. 171-173 °C; ^{1}H NMR (400 MHz, DMSO-d_6) δ 3.85 (s, 3H), 7.12 (d, ^{3}J = 9.0 Hz, 2H), 7.68 (t, ^{3}J = 7.8 Hz, 1H), 7.91 (d, ^{3}J = 8.9 Hz, 2H), 8.06 (dd, ^{3}J = 7.9, ^{4}J = 1.6 Hz, 2H), 8.32 (d, ^{4}J = 1.9 Hz, 1H), 13.25 (br s, 1H); ^{13}C NMR (100 MHz, DMSO-d_6) δ 56.1, 115.1, 122.4, 125.3, 127.5, 130.2, 131.6, 132.5, 146.5, 152.4, 162.8, 167.2. HRMS (ESI+) calc. for [M+H]$^{+}$ ($C_{14}H_{13}N_2O_3$): 257.0921, found: 257.0923.

***Trans*-2c: *Trans-N*-(3-methoxy-1H-pyrazolo[3,4-b]pyridin-5-yl)-3-((4-methoxyphenyl)-diazenyl)benzamide.**

A solution of compound **10** (0.60 mmol, 154 mg), 3-methoxy-1H-pyrazolo[3,4-b]pyridin-5-amine (0.55 mmol, 90 mg, prepared by a published procedure [52]) and EDC (0.60 mmol, 115 mg) in DMF (6 mL) was stirred at rt overnight. Afterwards, the reaction mixture was diluted with ethyl acetate (80 mL) and washed with brine (2 x 60 mL), 1N aq. HCl (60 mL), sat. aq. $NaHCO_3$ (60 mL) and again brine (60 mL). The organic phase was dried ($MgSO_4$). The volatiles were partially removed *in vacuo* and to the residue was added pentane (80 mL). The resulting precipitate was filtered to provide product as orange powder (110 mg, 50%). R_f = 0.38 (pentane/AcOEt, 1:1, v/v); Mp. = 233-235 °C; ^{1}H NMR (400 MHz, DMSO-d_6): δ 3.87 (s, 3H), 4.01 (s, 3H), 7.15 (d, ^3J = 8.9 Hz, 2H), 7.74 (t, ^3J = 7.8 Hz, 1H), 7.95 (d, ^3J = 8.9 Hz, 2H), 8.04 (d, ^3J = 7.9 Hz, 1H), 8.11 (d, ^3J = 8.1 Hz, 1H), 8.44 (s, 1H), 8.49 (d, ^4J = 2.3 Hz, 1H), 8.74 (d, ^4J = 2.3 Hz, 1H), 10.65 (s, 1H), 12.52 (s, 1H). ^{13}C NMR (100 MHz, DMSO-d_6): δ 56.0, 56.1, 102.9, 115.2, 120.1, 121.9, 125.2, 125.5, 128.9, 130.1, 130.2, 136.2, 145.3, 146.6, 150.1, 152.4, 155.0, 162.8, 165.5. HRMS (ESI+) calc. for $[M+H]^+$ ($C_{21}H_{19}N_6O_3$): 403.1513, found: 403.1502.

***Cis*-2c:**

A solution of compound ***trans*-2c** in DMSO-d6 (0.5 mL, ~1 mg/mL) was irradiated at λ = 365 nm (distance ~1 cm) to provide a sample of 94% ***cis*-2c**. ^{1}H NMR (400 MHz, DMSO-d_6): δ 3.71 (s, 3H), 3.99 (s, 3H), 6.78 – 7.11 (m, 4H), 7.46 (t, ^3J = 7.8 Hz, 1H), 7.61 (t, ^4J = 1.9 Hz, 1H), 7.79 (d, ^3J = 7.4 Hz, 1H), 8.44 (d, ^4J = 2.3 Hz, 1H), 8.68 (d, ^4J = 2.4 Hz, 1H), 10.48 (s, 1H), 12.51 (s, 1H).

11: Methyl 2,6-difluoro-3-(2-fluoro-phenyldiazenyl)benzoate.

A solution of methyl 3-amino-2,6-difluorobenzoate (5.00 mmol, 935 mg, Combi-Blocks) and 2-fluoro-nitrosobenzene (4.24 mmol, 530 mg, prepared according to a published procedure [53]) in acetic acid (15 mL) was heated at 40 °C overnight. Afterwards, the reaction mixture was diluted with diethyl ether (100 mL) and washed with 1N aq. HCl (2 x 80 mL), sat. aq. $NaHCO_3$ (80 mL) and brine (80 mL). The organic phase was dried ($MgSO_4$) and filtered through a plug of silica. The volatiles were removed *in vacuo* and to the residue was added pentane (100 mL). The resulting suspension was filtered and the volatiles were removed to provide product as red powder (700 mg, 56%). R_f = 0.66 (pentane/Et_2O, 4:1, v/v); Mp. 92-93 °C; ^{1}H NMR (400 MHz, $CDCl_3$): δ 4.02 (s, 3H), 7.04 (td, *J* = 9.0, 1.7 Hz, 1H), 7.18 – 7.34 (m, 2H), 7.50 (dddd, *J* = 8.7, 6.9, 5.0, 1.8 Hz, 1H), 7.79 (td, *J* = 7.8, 1.8 Hz, 1H), 7.96 (ddd, *J* = 9.2, 8.1, 5.9 Hz, 1H). ^{13}C NMR (100 MHz, $CDCl_3$): δ 53.04 , 112.3 (dd, *J* = 23.3, 4.1 Hz), 117.1 (d, *J* = 19.7 Hz), 117.7 , 121.0 (dd, *J* = 10.8, 1.9 Hz), 124.4 (d, *J* = 3.8 Hz), 130.0 (d, *J* = 7.4 Hz), 133.5 (d, *J* = 8.4 Hz), 137.7 (dd, *J* = 7.1, 4.3 Hz), 140.5 (d, *J* = 6.7 Hz), 158.5 (dd, *J* = 269.0, 6.7 Hz), 159.2 , 161.8 , 162.2 (dd, *J* = 262.7, 5.9 Hz); ^{19}F NMR (376 MHz, $CDCl_3$): -104.8 (m), -120.1 (m), -123.8 (m); HRMS (ESI+) calc. for $[M+H]^+$ ($C_{14}H_{10}F_3N_2O_2$): 295.0689, found: 295.0688.

12: 2,6-difluoro-3-(2-fluoro-phenyldiazenyl)benzoic acid.

To a solution of compound **11** (1.77 mmol, 520 mg) in THF (15 mL) was added sat. aq. LiOH (10 mL). The resulting biphasic mixture was vigorously stirred for 5h, after which the volatiles were evaporated. 1N aq. HCl (30 mL) was added to the residue, the resulting precipitate was filtered off and redissolved in AcOEt (60 mL). The solution was dried ($MgSO_4$) and the volume was reduced. The product was precipitated by addition of pentane, filtered off and washed with pentane to give product (240 mg, 48%). Mp. 206-208 °C; ^{1}H NMR (400 MHz, DMSO-d_6): δ 7.29 – 7.39 (m, 1H), 7.49 (dd, *J* = 11.0, 8.3 Hz, 1H), 7.66 (dtd, *J* = 16.3, 7.9, 3.6 Hz, 2H), 7.85 (td, *J* = 8.8, 5.9 Hz, 1H); ^{13}C NMR (100 MHz, DMSO-d_6): δ 113.6 (dd, *J* = 23.5, 3.8 Hz), 117.8, 118.0, 120.9 (d, *J* = 10.9 Hz), 125.6 (d, *J* = 3.7 Hz), 134.9 (d, *J* = 8.5 Hz),

137.6 (d, *J* = 3.9 Hz), 140.2 (d, *J* = 6.9 Hz), 156.9 (*J* = 265.3, 7.5 Hz), 158.7, 161.3, 161.5 (dd, *J* = 258.6, 6.5 Hz), 161.9; ^{19}F NMR (376 MHz, DMSO-d_6): -106.1 (m), -122.3 (m), -124.0 (m); HRMS (ESI+) calc. for $[M+H]^+$ ($C_{13}H_8F_3N_2O_2$): 281.0532, found: 281.0533.

***Trans*-2d: *trans*-2,6-difluoro-3-((2-fluorophenyl)diazenyl)-N-(3-methoxy-1H-pyrazolo[3,4-b]pyridin-5-yl)benzamide.**

A solution of compound **12** (0.60 mmol, 168 mg), 3-methoxy-1H-pyrazolo[3,4-b]pyridin-5-amine (0.42 mmol, 70 mg, prepared by a published procedure [52]) and EDC (0.60 mmol, 115 mg) in DMF (5 mL) was stirred at rt overnight. Afterwards, the reaction mixture was diluted with ethyl acetate (80 mL) and washed with brine (2 x 60 mL) ,1N aq. HCl (2 x 60 mL), sat. aq. $NaHCO_3$ (60 mL) and again brine (60 mL). The organic phase was dried ($MgSO_4$). The volatiles were partially removed *in vacuo* and to the residue was added pentane (100 mL). The resulting precipitate was filtered to provide product as orange powder (63 mg, 35%). R_f = 0.46 (pentane/AcOEt, 1:1, v/v); Mp. >240 °C; ^{1}H NMR (400 MHz, DMSO-d_6): δ 4.01 (s, 3H), 7.38 (t, ^3J = 8.8 Hz, 1H), 7.45 (t, ^3J = 8.8 Hz, 1H), 7.54 (dd, *J* = 10.9, 8.4 Hz, 1H), 7.64 – 7.77 (m, 2H), 7.88 – 7.97 (m, 1H), 8.51 (d, ^4J = 2.3 Hz, 1H), 8.61 (d, ^4J = 2.4 Hz, 1H), 11.23 (s, 1H), 12.61 (s, 1H). ^{13}C NMR (100 MHz, DMSO-d_6): δ 56.1 , 102.9, 113.6 (d, J_{C-F} = 23.0 Hz), 117.8, 118.0, 119.0, 120.5, 125.6, 128.4, 135.0 (d, J_{C-F} = 8.3 Hz), 137.5 , 140.3 (d, J_{C-F} = 6.5 Hz), 143.9, 150.2, 155.1, 156.8 (dd, J_{C-F} = 261.7, 7.8 Hz), 157.9, 158.7, 161.1 (dd, J_{C-F} = 256.1, 6.7 Hz), 161.3; ^{19}F NMR (376 MHz, DMSO-d_6): -124.0 (m), -123.5 (m), -107.6 (m); HRMS (ESI+) calc. for $[M+H]^+$ ($C_{20}H_{14}F_3N_6O_2$): 427.1125, found: 427.1116.

***Cis*-2d:**

A solution of compound ***trans*-2d** in DMSO-d6 (0.5 mL, ~2 mg/mL) was irradiated at λ = 365 nm (distance ~1 cm) to provide a sample of 70% ***cis*-2d**. ^{1}H NMR (400 MHz, DMSO-d_6): δ 3.99 (s, 3H), 7.05-7.15 (m, 2H), 7.20-7.30 (m, 3H), 7.31-7.35 (m, 1H), 8.43 (d, ^4J = 2.4 Hz, 1H), 8.54 (d, ^4J = 2.0 Hz, 1H), 11.08 (s, 1H), 12.58 (s, 1H); ^{19}F NMR (376 MHz, DMSO-d_6): -123.3 (m), -122.5, -112.5 (m).

13: Methyl 2,6-difluoro-3-(*p*-tolyldiazenyl)benzoate.

A solution of methyl 3-amino-2,6-difluorobenzoate (5.00 mmol, 935 mg, Combi-Blocks) and 4-methyl-nitrosobenzene (4.24 mmol, 517 mg) in acetic acid (15 mL) was heated at 40 °C overnight. Afterwards, the reaction mixture was diluted with diethyl ether (150 mL) and washed with 1N aq. HCl (2 x 100 mL), sat. aq. $NaHCO_3$ (100 mL) and brine (100 mL). The organic phase was dried ($MgSO_4$) and the product was purified by flash chromatography (Silicagel, 40-63 µm, pentane:Et_2O, 9:1, v/v) to give orange powder (770 mg, 63%). R_f = 0.66 (pentane/Et_2O, 9:1, v/v); Mp. 98-100 °C; ^{1}H NMR (400 MHz, $CDCl_3$): δ 2.43 (s, 3H), 4.01 (s, 3H), 7.00 (td, J = 9.0, 1.7 Hz, 1H), 7.30 (d, ^3J = 8.1 Hz, 2H), 7.83 (d, ^3J = 8.3 Hz, 2H), 7.84 – 7.92 (m, 1H); ^{13}C NMR (100 MHz, $CDCl_3$): δ 21.5 , 53.0 , 112.2 (dd, $J_{C–F}$ = 23.1, 4.1 Hz), 120.9 (dd, $J_{C–F}$ = 10.7, 2.2 Hz), 123.3 , 129.8 , 137.6 (dd, $J_{C–F}$ = 7.3, 4.1 Hz), 142.6 , 150.7 , 158.0 (dd, $J_{C–F}$ = 267.9, 6.6 Hz), 161.6 (d, $J_{C–F}$ = 1.4 Hz), 161.6 (dd, $J_{C–F}$ = 261.3, 5.8 Hz); ^{19}F NMR (376 MHz, $CDCl_3$): -120.8 (dd, J = 8.7, 4.1 Hz), -106.5 (dd, J = 9.2, 4.1 Hz); HRMS (ESI+) calc. for $[M+H]^+$ ($C_{15}H_{13}F_2N_2O_2$): 291.0940, found: 291.0943.

14: 2,6-difluoro-3-(*p*-tolyldiazenyl)benzoic acid.

To a solution of compound **13** (1.79 mmol, 520 mg) in THF (15 mL) was added sat. aq. LiOH (10 mL). The resulting biphasic mixture was vigorously stirred overnight, after which the volatiles were evaporated. 1N aq. HCl (30 mL) was added to the residue, the resulting precipitate was filtered off and redissolved in THF (60 mL). The solution was dried ($MgSO_4$) and the volume was reduced. The product was precipitated by addition of pentane, filtered off and washed with pentane to give orange powder (390 mg, 79%). Mp. 209-211 °C; ^{1}H NMR (400 MHz, DMSO-d_6): δ 2.40 (s, 3H), 7.30 – 7.38 (m, 1H), 7.41 (d, ^3J = 6.5 Hz, 2H), 7.81 (d, ^3J = 6.4 Hz, 2H), 7.88 (tdd, J = 8.8, 6.1, 2.4 Hz, 1H); ^{13}C NMR (100 MHz, DMSO-d_6): δ 21.5 , 113.4 (dd, $J_{C–F}$ = 23.3, 3.8 Hz), 120.8 (d, $J_{C–F}$ = 11.1 Hz), 123.4 , 130.5 , 136.8 – 138.2 (m), 143.3 , 150.5 , 156.9 (dd, $J_{C–F}$ = 263.3, 7.6 Hz), 160.9 (dd, $J_{C–F}$ = 257.3, 6.7 Hz),

162.0; ^{19}F NMR (376 MHz, DMSO-d_6): -123.1 (dd, *J* = 8.8, 4.9 Hz), -107.6 (dt, *J* = 9.7, 5.5 Hz); HRMS (ESI+) calc. for $[M+H]^+$ ($C_{14}H_{11}F_2N_2O_2$): 277.0783, found: 277.0784.

***Trans*-2e: *trans*-2,6-difluoro-N-(3-methoxy-1H-pyrazolo[3,4-b]pyridin-5-yl)-3-(*p*-tolyldiazenyl)benzamide.**

A solution of compound **14** (0.60 mmol, 166 mg), 3-methoxy-1H-pyrazolo[3,4-b]pyridin-5-amine (0.42 mmol, 70 mg, prepared by a published procedure [52]) and EDC (0.60 mmol, 115 mg) in DMF (4 mL) was stirred at rt overnight. Afterwards, the reaction mixture was diluted with ethyl acetate (80 mL) and washed with brine (60 mL) ,1N aq. HCl (2 x 60 mL), sat. aq. $NaHCO_3$ (60 mL) and again brine (2 x 60 mL). The organic phase was dried ($MgSO_4$). The volatiles were partially removed *in vacuo* and to the residue was added pentane (100 mL). The resulting precipitate was filtered to provide product as orange powder (115 mg, 64%). R_f = 0.57 (pentane/AcOEt, 1:1, v/v); Mp. >220 °C; ^{1}H NMR (400 MHz, DMSO-d_6): 2.41 (s, 3H), 4.01 (s, 3H), 7.26 – 7.52 (m, 3H), 7.83 (dd, *J* = 8.3, 1.5 Hz, 2H), 7.92 (q, *J* = 8.4 Hz, 1H), 8.52 (s, 1H), 8.61 (s, 1H), 11.21 (s, 1H), 12.61 (s, 1H); ^{13}C NMR (100 MHz, DMSO-d_6): δ 21.5, 56.1, 102.9, 113.3 (dd, J_{C-F} = 23.1, 3.6 Hz), 116.7 (dd, J_{C-F} = 23.6, 21.0 Hz), 118.9, 120.3 (d, J_{C-F} = 10.6 Hz), 123.4, 128.4, 130.5, 137.3 (dd, J_{C-F} = 7.2, 3.8 Hz), 143.3, 143.8, 150.1, 150.6, 155.1, 156.5 (dd, J_{C-F} = 260.1, 8.1 Hz), 158.1, 160.6 (dd, J_{C-F} = 254.5, 7.2 Hz); ^{19}F NMR (376 MHz, DMSO-d_6): -124.2 (t, *J* = 6.8 Hz), -109.1 (q, *J* = 7.3, 6.6 Hz); HRMS (ESI+) calc. for $[M+H]^+$ ($C_{21}H_{17}F_2N_6O_2$): 423.1376, found: 423.1331.

***Cis*-2e:**

A solution of compound ***trans*-2e** in DMSO-d_6 (0.5 mL, ~2 mg/mL) was irradiated at λ = 365 nm (distance ~1 cm) to provide a sample of 84% ***cis*-2e**. ^{1}H NMR (400 MHz, DMSO-d_6): δ 2.27 (s, 3H), 3.99 (s, 3H), 6.87 (d, *J* = 8.2 Hz, 2H), 7.10 (td, *J* = 8.5, 5.8 Hz, 1H), 7.17 – 7.28 (m, 3H), 8.43 (d, *J* = 2.4 Hz, 1H), 8.55 (d, *J* = 2.3 Hz, 1H), 11.05 (s, 1H), 12.58 (s, 1H). ^{19}F NMR (376 MHz, DMSO-d_6): -122.8 (dd, *J* = 8.5, 3.6 Hz), -114.4 (dq, *J* = 8.9, 3.9 Hz).

15: Methyl 2,6-difluoro-3-((4-fluorophenyl)diazenyl)benzoate.

A solution of methyl 3-amino-2,6-difluorobenzoate (3.96 mmol, 741 mg, Combi-Blocks) and 4-fluoro-nitrosobenzene (3.28 mmol, 410 mg) in acetic acid (10 mL) was heated at 40 °C overnight. Afterwards, the reaction mixture was diluted with diethyl ether (100 mL) and washed with 1N aq. HCl (2 x 70 mL), sat. aq. $NaHCO_3$ (70 mL) and brine (70 mL). The organic phase was dried ($MgSO_4$) and the product was purified by flash chromatography (Silicagel, 40-63 μm, pentane:Et_2O, 9:1, v/v) to give orange powder (382 mg, 40%). R_f = 0.42 (pentane/Et_2O, 9:1, v/v); Mp. 68-70 °C; ^{1}H NMR (400 MHz, $CDCl_3$): δ 4.01 (s, 3H), 6.95 – 7.06 (m, 1H), 7.13 – 7.24 (m, 2H), 7.81 – 7.91 (m, 1H), 7.90 – 7.97 (m, 2H); ^{13}C NMR (100 MHz, $CDCl_3$): δ 53.0, 112.2 (dd, $J_{C–F}$ = 23.2, 4.2 Hz), 116.2 (d, $J_{C–F}$ = 23.0 Hz), 120.8 (dd, $J_{C–F}$ = 10.7, 2.1 Hz), 125.3 (d, $J_{C–F}$ = 9.0 Hz), 137.3 (dd, $J_{C–F}$ = 7.2, 4.3 Hz), 149.0 (d, $J_{C–F}$ = 3.1 Hz), 158.2 (dd, $J_{C–F}$ = 268.4, 6.6 Hz), 161.4 , 161.8 (dd, $J_{C–F}$ = 262.0, 5.8 Hz), 163.6, 166.1. ^{19}F NMR (376 MHz, $CDCl_3$): -120.5 (dd, J = 8.2, 4.4 Hz), -107.7 , -106.5 – -104.9 (m); HRMS (ESI+) calc. for $[M+H]^+$ ($C_{14}H_{10}F_3N_2O_2$): 295.0689, found: 295.0664.

16: 2,6-difluoro-3-((4-fluorophenyl)diazenyl)benzoic acid.

To a solution of compound **15** (1.23 mmol, 361 mg) in THF (12 mL) was added sat. aq. LiOH (8 mL). The resulting biphasic mixture was vigorously stirred overnight, after which the volatiles were evaporated. 1N aq. HCl (30 mL) was added to the residue, the resulting precipitate was filtered off and redissolved in THF (60 mL). The solution was dried ($MgSO_4$) and the volume was reduced. The product was precipitated by addition of pentane, filtered off and washed with pentane to give orange powder (230 mg, 67%). The crude product was used in the next step without further characterization.

***Trans*-2f: *trans*-2,6-difluoro-N-(3-methoxy-1H-pyrazolo[3,4-b]pyridin-5-yl)-3-((4-fluoro-phenyl)diazenyl)benzamide.**

A solution of compound **16** (0.60 mmol, 170 mg), 3-methoxy-1H-pyrazolo[3,4-b]pyridin-5-amine (0.42 mmol, 70 mg, prepared by a published procedure [52]) and EDC (0.60 mmol, 115 mg) in DMF (4 mL) was stirred at rt overnight. Afterwards, the reaction mixture was diluted with ethyl acetate (80 mL) and washed with brine (60 mL) ,1N aq. HCl (2 x 60 mL), sat. aq. $NaHCO_3$ (60 mL) and again brine (2 x 60 mL). The organic phase was dried ($MgSO_4$). The volatiles were partially removed *in vacuo* and to the residue was added pentane (100 mL). The resulting precipitate was filtered to provide product as orange powder (100 mg, 56%). R_f = 0.70 (pentane/AcOEt, 1:1, v/v); Mp. >220 °C; ^{1}H NMR (400 MHz, DMSO-d_6): δ 4.01 (s, 3H), 7.29 – 7.54 (m, 3H), 7.73 – 8.04 (m, 3H), 8.53 (d, ^4J = 2.4 Hz, 1H), 8.63 (d, ^4J = 2.4 Hz, 1H), 11.23 (s, 1H), 12.61 (s, 1H); ^{13}C NMR (100 MHz, DMSO-d_6): δ 56.1, 102.9, 113.4 (d, $J_{C–F}$ = 20.8 Hz), 117.1 (d, $J_{C–F}$ = 23.2 Hz), 118.9, 120.4 (d, $J_{C–F}$ = 10.6 Hz), 125.8 (d, $J_{C–F}$ = 9.4 Hz), 128.4, 137.2, 143.8, 149.2 (d, $J_{C–F}$ = 2.9 Hz), 150.1, 155.1, 156.6 (dd, $J_{C–F}$ = 260.8, 8.0 Hz), 158.0, 160.8 (dd, $J_{C–F}$ = 255.2, 7.1 Hz), 163.5, 166.0; ^{19}F NMR (376 MHz, DMSO-d_6): -124.3 – -123.1 (m), -108.4 (d, J = 7.0 Hz), -108.1 – -106.7 (m); HRMS (ESI+) calc. for $[M+H]^+$ ($C_{20}H_{13}F_3N_6O_2Na$): 449.0944, found: 449.0893.

***Cis*-2f:**

A solution of compound ***trans*-2f** in DMSO-d_6 (0.5 mL, ~2 mg/mL) was irradiated at λ = 365 nm (distance ~1 cm) to provide a sample of 62% ***cis*-2f**. ^{1}H NMR (400 MHz, DMSO-d_6): 3.99 (s, 3H), 7.00 – 7.10 (m, 2H), 7.17 (td, J = 8.5, 5.9 Hz, 1H), 7.25 (t, J = 8.8 Hz, 2H), 7.46 (t, J = 8.7 Hz, 1H), 8.42 (d, J = 2.4 Hz, 1H), 8.54 (d, J = 2.4 Hz, 1H), 11.04 (s, 1H), 12.58 (s, 1H); δ ^{19}F NMR (376 MHz, DMSO-d_6): -122.2 (dd, J = 8.1, 4.0 Hz), -113.8 (dt, J = 9.0, 4.8 Hz), -112.5 (dt, J = 8.7, 4.1 Hz).

17: Methyl 2,6-difluoro-3-(*o*-tolyldiazenyl)benzoate.

A solution of methyl 3-amino-2,6-difluorobenzoate (5.00 mmol, 935 mg, Combi-Blocks) and 2-methyl-nitrosobenzene (4.24 mmol, 517 mg) in acetic acid (10 mL) was heated at 40 °C overnight. Afterwards, the reaction mixture was diluted with diethyl ether (150 mL) and washed with 1N aq. HCl (2 x 100 mL), sat. aq. $NaHCO_3$ (100 mL) and brine (100 mL). The

organic phase was dried ($MgSO_4$) and the product was purified by precipitation from Et_2O/pentane to give red crystals (410 mg, 33%). R_f = 0.80 (pentane/Et_2O, 9:1, v/v); Mp. 87-89 °C; ^{1}H NMR (400 MHz, $CDCl_3$) δ 2.72 (s, 3H), 4.02 (s, 3H), 7.03 (td, *J* = 8.9, 1.7 Hz, 1H), 7.24 – 7.30 (m, 1H), 7.32 – 7.43 (m, 2H), 7.67 (dd, *J* = 8.1, 1.3 Hz, 1H), 7.87 (ddd, *J* = 9.1, 8.2, 6.0 Hz, 1H). ^{19}F NMR (376 MHz, $CDCl_3$) δ -120.8 (dd, *J* = 8.4, 4.0 Hz), -106.3 (dt, *J* = 9.5, 5.0 Hz). ^{13}C NMR (101 MHz, $CDCl_3$) δ 17.5, 53.0, 112.2 (dd, *J* = 23.2, 4.2 Hz), 115.8, 121.1 (dd, *J* = 10.7, 2.3 Hz), 126.5, 131.4, 131.8, 137.9 (dd, *J* = 7.2, 4.2 Hz), 138.8, 150.6, 158.1 (dd, *J* = 268.2, 6.7 Hz), 161.6 (d, *J* = 1.2 Hz), 161.7 (dd, *J* = 261.5, 5.9 Hz). HRMS (ESI+) calc. for $[M+H]^+$ ($C_{15}H_{13}F_2N_2O_2$): 291.0940, found: 291.0916.

18: 2,6-difluoro-3-(*o*-tolyldiazenyl)benzoic acid.

To a solution of compound **17** (1.36 mmol, 375 mg) in THF (12 mL) was added sat. aq. LiOH (8 mL). The resulting biphasic mixture was vigorously stirred overnight, after which the volatiles were evaporated. 1N aq. HCl (30 mL) was added to the residue, the resulting precipitate was filtered off and redissolved in THF (60 mL). The solution was dried ($MgSO_4$) and the volume was reduced. The product was precipitated by addition of pentane, filtered off and washed with pentane to give orange powder (230 mg, 61%). Mp. 170-171 °C; ^{1}H NMR (400 MHz, DMSO-d_6) δ 2.65 (s, 3H), 7.28 – 7.37 (m, 2H), 7.38 – 7.50 (m, 2H), 7.53 (d, *J* = 8.0 Hz, 1H), 7.87 (td, *J* = 8.8, 6.1 Hz, 1H). ^{19}F NMR (376 MHz, DMSO-d_6) δ -123.2 (dd, *J* = 8.4, 5.0 Hz), -107.4 (dt, *J* = 10.4, 5.4 Hz). ^{13}C NMR (101 MHz, DMSO-d_6) δ 17.5, 113.4 (dd, *J* = 23.2, 3.9 Hz), 113.7 – 114.2 (m), 115.7, 121.2 (d, *J* = 10.5 Hz), 127.2, 132.0, 132.7, 137.7 (dd, *J* = 7.1, 3.9 Hz), 138.9, 150.4, 157.0 (dd, *J* = 263.6, 7.6 Hz), 161.0 (dd, *J* = 257.6, 6.6 Hz), 162.0. HRMS (ESI+) calc. for $[M+H]^+$ ($C_{14}H_{11}F_2N_2O_2$): 277.0783, found: 277.0761.

***Trans*-2g: *trans*-2,6-difluoro-*N*-(3-methoxy-1H-pyrazolo[3,4-b]pyridin-5-yl)-3-(*o*-tolyldiazenyl)benzamide.**

A solution of compound **18** (0.60 mmol, 166 mg), 3-methoxy-1H-pyrazolo[3,4-b]pyridin-5-amine (0.42 mmol, 70 mg, prepared by a published procedure [52]) and EDC (0.60 mmol, 115 mg) in DMF (4 mL) was stirred at rt overnight. Afterwards, the reaction mixture was diluted with ethyl acetate (80 mL) and washed with brine (60 mL) ,1N aq. HCl (2 x 60 mL), sat. aq. $NaHCO_3$ (60 mL) and again brine (2 x 60 mL). The organic phase was dried ($MgSO_4$). The volatiles were partially removed *in vacuo* and to the residue was added pentane (100 mL). The resulting precipitate was filtered to provide product as orange powder (116 mg, 65%). R_f = 0.73 (pentane/AcOEt, 1:1, v/v); Mp. >220 °C; ^{1}H NMR (400 MHz, DMSO-d_6) δ 2.68 (s, 3H), 4.01 (s, 3H), 7.28 – 7.38 (m, 1H), 7.38 – 7.52 (m, 3H), 7.56 (d, *J* = 8.1 Hz, 1H), 7.93 (td, *J* = 8.4, 5.5 Hz, 1H), 8.53 (d, *J* = 2.3 Hz, 1H), 8.63 (d, *J* = 1.1 Hz, 1H), 11.22 (s, 1H), 12.61 (s, 1H). ^{19}F NMR (376 MHz, DMSO-d_6) δ -124.3 (dd, *J* = 8.4, 5.5 Hz), -108.9 (q, *J* = 7.1, 6.6 Hz); ^{13}C NMR (101 MHz, DMSO-d_6) δ 17.6, 56.1, 102.9, 113.4 (d, *J* = 23.0 Hz), 115.7, 116.7 (dd, *J* = 23.4, 20.9 Hz), 118.9, 120.7 (d, *J* = 10.5 Hz), 127.2, 128.4, 132.1, 132.7, 137.7 (d, *J* = 7.1 Hz), 138.9, 143.9, 150.2, 150.5, 155.1, 156.5 (dd, *J* = 260.7, 8.3 Hz), 158.1, 160.6 (dd, *J* = 254.4, 7.0 Hz). HRMS (ESI+) calc. for $[M+H]^+$ ($C_{21}H_{17}F_2N_6O_2$): 423.1376, found: 423.1371.

***Cis*-2g:** A solution of compound ***trans*-2g** in DMSO-d_6 (0.5 mL, ~2 mg/mL) was irradiated at λ = 365 nm (distance ~1 cm) to provide a sample of 77% ***cis*-2g**. ^{1}H NMR (400 MHz, DMSO-d_6): δ 2.28 (s, 3H), 3.99 (s, 3H), 6.26 – 6.45 (m, 1H), 7.02 – 7.11 (m, 2H), 7.15-7.25 (m, 2H), 7.31 (d, *J* = 7.6 Hz, 1H), 8.43 (d, *J* = 2.4 Hz, 1H), 8.55 (d, *J* = 2.4 Hz, 1H), 11.06 (s, 1H), 12.58 (s, 1H).^{19}F NMR (376 MHz, DMSO-d_6) δ -123.0 (dd, *J* = 8.2, 4.1 Hz), -113.8 (dq, *J* = 8.9, 5.1, 4.5 Hz).

19: Methyl 2,6-difluoro-3-((2-fluorophenyl)diazenyl)benzoate. A solution of methyl 3-amino-2,6-difluorobenzoate (6.00 mmol, 1.12 g, Combi-Blocks) and 2-methoxy-nitrosobenzene (5.10 mmol, 700 mg) in acetic acid (16 mL) was heated at 40 °C overnight. Afterwards, the reaction mixture was diluted with diethyl ether (100 mL) and washed with 1N

aq. HCl (2 x 70 mL), sat. aq. $NaHCO_3$ (70 mL) and brine (70 mL). The organic phase was dried ($MgSO_4$) and the product was purified by flash chromatography (Silicagel, 40-63 µm, pentane:Et_2O, 9:1, v/v) to give orange powder (205 mg, 13%). R_f = 0.70 (pentane/Et_2O, 1:1, v/v); Mp. 93-95 °C; ^{1}H NMR (400 MHz, $CDCl_3$) δ 4.00 (s, 3H), 4.02 (s, 3H), 6.97 – 7.04 (m, 2H), 7.09 (dd, *J* = 8.4, 1.1 Hz, 1H), 7.47 (ddd, *J* = 8.8, 7.3, 1.7 Hz, 1H), 7.70 (dd, *J* = 8.0, 1.7 Hz, 1H), 7.89 (ddd, *J* = 9.1, 8.2, 6.0 Hz, 1H). ^{19}F NMR (376 MHz, $CDCl_3$) δ -120.8 (ddd, *J* = 8.2, 4.1, 2.0 Hz), -106.4 (td, *J* = 5.8, 3.0 Hz). ^{13}C NMR (101 MHz, $CDCl_3$) δ 53.0 , 56.3 , 111.9 (d, *J* = 2.1 Hz), 112.2 (dd, *J* = 23.0, 4.2 Hz), 112.8, 117.1, 120.8, 121.4 (dd, *J* = 10.7, 2.2 Hz), 133.5, 138.1 (dd, *J* = 7.3, 4.2 Hz), 142.1, 157.5, 158.0 (dd, *J* = 268.0, 6.5 Hz), 161.6 (d, *J* = 1.3 Hz), 161.6 (dd, *J* = 261.4, 5.8 Hz). HRMS (ESI+) calc. for $[M+H]^+$ ($C_{15}H_{13}F_3N_2O_3$): 307.0888, found: 307.0888.

20: 2,6-difluoro-3-((4-fluorophenyl)diazenyl)benzoic acid. To a solution of compound **19** (0.65 mmol, 200 mg) in THF (4 mL) was added sat. aq. LiOH (4 mL). The resulting biphasic mixture was vigorously stirred overnight, after which the volatiles were evaporated. 1N aq. HCl (30 mL) was added to the residue, the resulting precipitate was filtered off and redissolved in THF (60 mL). The solution was dried ($MgSO_4$) and the volume was reduced. The product was precipitated by addition of pentane, filtered off and washed with pentane to give orange powder. The crude product was used in the next step without further characterization.

***Trans*-2h: *trans*-2,6-difluoro-N-(3-methoxy-1H-pyrazolo[3,4-b]pyridin-5-yl)-3-((4-fluoro-phenyl)diazenyl)benzamide.** A solution of crude compound **20**, 3-methoxy-1H-pyrazolo[3,4-b]pyridin-5-amine (0.42 mmol, 70 mg, prepared by a published procedure [52]) and EDC (0.54 mmol, 104 mg) in DMF (4 mL) was stirred at rt overnight. Afterwards, the reaction mixture was diluted with ethyl acetate (80 mL) and washed with brine (60 mL) ,1N aq. HCl (2 x 60 mL), sat. aq. $NaHCO_3$ (60 mL) and again brine (2 x 60 mL). The organic phase was

dried ($MgSO_4$). The volatiles were partially removed *in vacuo* and to the residue was added pentane (100 mL). The resulting precipitate was filtered to provide product as orange powder (78 mg, 40% from **19**). R_f = 0.47 (pentane/AcOEt, 1:1, v/v); Mp. >220 °C; ^{1}H NMR (400 MHz, DMSO-d_6) δ 3.97 (s, 3H), 4.01 (s, 3H), 7.05 (t, *J* = 7.6 Hz, 1H), 7.29 (d, *J* = 8.3 Hz, 1H), 7.36 – 7.46 (m, 1H), 7.52 – 7.61 (m, 2H), 7.84 (td, *J* = 8.8, 6.1 Hz, 1H), 8.53 (d, *J* = 2.3 Hz, 1H), 8.63 (d, *J* = 2.3 Hz, 1H), 11.22 (s, 1H), 12.61 (s, 1H). ^{19}F NMR (376 MHz, DMSO-d_6) δ -124.4 (dd, *J* = 8.7, 5.2 Hz), -109.3 (app q, *J* = 6.2 Hz). ^{13}C NMR (101 MHz, DMSO-d_6) δ 56.1, 56.5, 102.9, 113.4 (dd, *J* = 23.0, 3.6 Hz), 114.1, 116.7 (dd, *J* = 23.5, 21.2 Hz), 116.8, 118.9, 120.5 (d, *J* = 10.4 Hz), 121.1, 128.4, 134.6, 137.8 (dd, *J* = 7.2, 3.8 Hz), 141.8, 143.9, 150.1, 155.1 (d, *J* = 6.4 Hz), 157.7, 157.8 (dd, *J* = 258.6, 6.6 Hz), 158.1, 160.4 (dd, *J* = 254.3, 7.1 Hz). HRMS (ESI+) calc. for $[M+H]^+$ ($C_{21}H_{17}F_2N_6O_3$): 439.1324, found: 439.1319.

***Cis*-2h:** A solution of compound ***trans*-2h** in DMSO-d_6 (0.5 mL, ~2 mg/mL) was irradiated at λ = 365 nm (distance ~1 cm) to provide a sample of 88% ***cis*-2h**. ^{1}H NMR (400 MHz, DMSO-d_6) δ 3.62 (s, 3H), 4.00 (s, 3H), 6.84 (app q, *J* = 8.1 Hz, 1H), 6.90 – 7.03 (m, 3H), 7.12 (t, *J* = 8.7 Hz, 1H), 7.19 – 7.28 (m, 1H), 8.44 (d, *J* = 2.3 Hz, 1H), 8.56 (dd, *J* = 2.4, 1.0 Hz, 1H), 11.06 (s, 1H), 12.58 (s, 1H). ^{19}F NMR (376 MHz, DMSO-d_6) δ -123.3 (dd, *J* = 8.2, 4.0 Hz), -114.0 (dt, *J* = 9.1, 4.6 Hz).

22: 2,6-difluoro-3-(phenylsulfonamido)benzoic acid. To a solution of methyl 3-amino-2,6-difluorobenzoate (3.00 mmol, 561 mg, Combi-Blocks) and benzenesulfonyl chloride (8.00 mmol, 1.02 mL) in DCM (15 mL) was added DMAP (30 mg) and triethylamine (10.0 mmol, 1.38 mL). The resulting mixture was stirred at rt for 20 h, after which it was diluted with Et_2O (100 mL) and washed with 1N HCl (2 x 80 mL), sat. aq. $NaHCO_3$ (80 mL) and brine (80 mL). The organic phase was dried ($MgSO_4$) and the solvent was partially evaporated *in vacuo*. Addition of pentane resulted in the precipitation of product **21**, which was used in the next step without further purification. Compound **21** (1.37 mmol, 640 mg) was stirred at rt for 2h in a mixture of 2N aq. KOH (10 mL), THF (24 mL) and methanol (6 mL). The reaction mixture was diluted with AcOEt (80 mL) and 1N HCl (80 mL). The aqueous phase was separated and extracted with AcOEt (80 mL). The combined organic fractions were washed with brine (100 mL). The organic phase was dried ($MgSO_4$) and the solvent was partially evaporated *in vacuo*. Addition of pentane resulted in the precipitation of product **22** as a light pink solid (420 mg, 83% over two steps). Mp. 144-145 °C; ^{1}H NMR (400 MHz, CD_3OD) δ 7.00 (t, J = 9.1, 1H), 7.43 – 7.64 (m, 4H), 7.73 (d, J = 7.3 Hz, 2H). ^{19}F NMR (376 MHz, CD_3OD) δ -123.31 (d, J = 8.7 Hz), -115.64 (t, J = 7.3 Hz). ^{13}C NMR (101 MHz, CD_3OD) δ 111.5 (dd, J = 23.0, 4.2 Hz), 121.6 (dd, J = 13.7, 4.0 Hz), 126.7, 128.8, 129.1 (dd, J = 10.1, 2.4 Hz), 132.8, 139.6, 152.0 (d, J = 7.1 Hz), 154.6 (d, J = 7.2 Hz), 156.2 (d, J = 5.8 Hz), 158.7 (d, J = 5.8 Hz), 162.2. HRMS (ESI+) calc. for $[M+Na]^+$ ($C_{13}H_9F_2NO_4SNa$): 336.0113, found: 336.0114.

1: 2,6-difluoro-N-(3-methoxy-1H-pyrazolo[3,4-b]pyridin-5-yl)-3-(phenylsulfonamido)-benzamide. [43]

A solution of compound **22** (0.60 mmol, 188 mg), 3-methoxy-1H-pyrazolo[3,4-b]pyridin-5-amine (0.42 mmol, 70 mg, prepared by a published procedure [52]), DMAP (10 mg) and EDC (0.60 mmol, 115 mg) in DMF (4 mL) was stirred at rt overnight. Afterwards, the reaction mixture was diluted with ethyl acetate (80 mL) and washed with brine (60 mL) ,1N aq. HCl (2 x 60 mL), sat. aq. $NaHCO_3$ (60 mL) and again brine (2 x 60 mL). The organic phase was dried ($MgSO_4$). The volatiles were partially removed *in vacuo* and to the residue was added pentane (100 mL). The resulting precipitate was filtered to provide product as white powder (25 mg, 13%). R_f = 0.20 (pentane/AcOEt, 1:1, v/v); Mp. >200 °C; ^{1}H NMR (400 MHz, DMSO-d6) δ 3.99 (s, 3H), 7.19 (t, *J* = 8.8 Hz, 1H), 7.33 (q, *J* = 8.2 Hz, 1H), 7.62 (m, 3H), 7.75 (d, *J* = 7.7 Hz, 2H), 8.42 (s, 1H), 8.53 (d, *J* = 2.4 Hz, 1H), 10.34 (s, 1H), 11.00 (s, 1H), 12.57 (s, 1H). ^{19}F NMR (376 MHz, DMSO-d6) δ -122.21, -116.18. HRMS (ESI+) calc. for $[M+H]^+$ ($C_{20}H_{16}F_2N_5O_4S$): 460.8856, found: 460.8816.

References

[1] https://www.kwf.nl/kanker/Pages/default.aspx, Dutch Cancer Soc. (2018).

[2] S. Ugurel, J. Röhmel, P.A. Ascierto, K.T. Flaherty, J.J. Grob, A. Hauschild, J. Larkin, G. V. Long, P. Lorigan, G.A. McArthur, A. Ribas, C. Robert, D. Schadendorf, C. Garbe, Survival of patients with advanced metastatic melanoma: The impact of novel therapies, Eur. J. Cancer. 53 (2016) 125–134. doi:10.1016/j.ejca.2015.09.013.

[3] H. Davies, G.R. Bignell, C. Cox, P. Stephens, S. Edkins, S. Clegg, J. Teague, H. Woffendin, M.J. Garnett, W. Bottomley, N. Davis, E. Dicks, R. Ewing, Y. Floyd, K. Gray, S. Hall, R. Hawes, J. Hughes, V. Kosmidou, A. Menzies, C. Mould, A. Parker, C. Stevens, S. Watt, S. Hooper, R. Wilson, H. Jayatilake, B.A. Gusterson, C. Cooper, J. Shipley, D. Hargrave, K. Pritchard-Jones, N. Maitland, G. Chenevix-Trench, G.J. Riggins, D.D. Bigner, G. Palmieri, A. Cossu, A. Flanagan, A. Nicholson, J.W.C. Ho, S.Y. Leung, S.T. Yuen, B.L. Weber, H.F. Seigler, T.L. Darrow, H. Paterson, R. Marais, C.J. Marshall, R. Wooster, M.R. Stratton, P.A. Futreal, 6-Mutations of the BRAF gene in human cancer., Nature. 417 (2002) 949–54. doi:10.1038/nature00766.

[4] A.X. Wang, X.Y. Qi, Targeting RAS/RAF/MEK/ERK signaling in metastatic melanoma, IUBMB Life. 65 (2013) 748–758. doi:10.1002/iub.1193.

[5] T. Rajakulendran, M. Sahmi, M. Lefrançois, F. Sicheri, M. Therrien, A dimerization-dependent mechanism drives RAF catalytic activation, Nature. 461 (2009) 542–545. doi:10.1038/nature08314.

[6] J. Yuan, W.H. Ng, P.Y.P. Lam, Y. Wang, H. Xia, J. Yap, S.P. Guan, A.S.G. Lee, M. Wang, M. Baccarini, J. Hu, The dimer-dependent catalytic activity of RAF family kinases is revealed through characterizing their oncogenic mutants, Oncogene. (2018) 1–16. doi:10.1038/s41388-018-0365-2.

[7] E. Desideri, A.L. Cavallo, M. Baccarini, Alike but Different: RAF Paralogs and Their Signaling Outputs, Cell. 161 (2015) 967–970. doi:10.1016/j.cell.2015.04.045.

[8] P.T.C. Wan, M.J. Garnett, S.M. Roe, S. Lee, D. Niculescu-duvaz, V.M. Good, C.G. Project, C.M. Jones, C.J. Marshall, C.J. Springer, D. Barford, R. Marais, Mechanism of Activation of the RAF-ERK Signaling Pathway by Oncogenic Mutations of B-RAF, 116 (2004) 855–867.

[9] G. Kim, A.E. McKee, Y.M. Ning, M. Hazarika, M. Theoret, J.R. Johnson, Q.C. Xu, S. Tang, R. Sridhara, X. Jiang, K. He, D. Roscoe, W. David McGuinn, W.S. Helms, A.M. Russell, S.P. Miksinski, J.F. Zirkelbach, J. Earp, Q. Liu, A. Ibrahim, R. Justice, R. Pazdur, FDA approval summary: Vemurafenib for treatment of unresectable or metastatic melanoma with the BRAFV600E mutation mutation, Clin. Cancer Res. 20 (2014) 4994–5000. doi:10.1158/1078-0432.CCR-14-0776.

[10] P. Rutkowski, C. Blank, Dabrafenib for the treatment of *BRAF* V600-positive melanoma: a safety evaluation, Expert Opin. Drug Saf. 13 (2014) 1249–1258. doi:10.1517/14740338.2014.939954.

[11] J.M. Chalovich, E. Eisenberg, Targeting raf kinases for cancer therapty, Magn Reson Imaging. 31 (2013) 477–479. doi:10.1016/j.immuni.2010.12.017.Two-stage.

[12] C.H. Adelmann, G. Ching, L. Du, R.C. Saporito, V. Bansal, L.J. Pence, R. Liang, W. Lee, K.Y. Tsai, Comparative profiles of BRAF inhibitors: the paradox index as a predictor of clinical toxicity, Oncotarget. 7 (2016). doi:10.18632/oncotarget.8351.

[13] S.F. Chandrakumar, J. Yeung, Cutaneous adverse events during vemurafenib therapy, J Cutan Med Surg. 18 (2014) 223–228. doi:10.2310/7750.2013.13120.

[14] W.A. Velema, W. Szymanski, B.L. Feringa, Photopharmacology : Beyond Proof of Principle, J. Am. Chem. Soc. 136 (2014) 2178–2191.

[15] J. Broichhagen, J.A. Frank, D. Trauner, A Roadmap to Success in Photopharmacology, Acc. Chem. Res. 48 (2015) 1947–1960.

[16] M.M. Lerch, M.J. Hansen, G.M. Van Dam, W. Szymanski, B.L. Feringa, Emerging Targets in Photopharmacology, Angew. Chem. Int. Ed. 55 (2016) 10978–10999.

[17] K. Hüll, J. Morstein, D. Trauner, In Vivo Photopharmacology, Chem. Rev. 118 (2018) 10710–10747.

[18] M.J. Hansen, W.A. Velema, M.M. Lerch, W. Szymanski, B.L. Feringa, Wavelength-selective cleavage of photoprotecting groups: strategies and applications in dynamic systems, Chem. Soc. Rev. 44 (2015) 3358–3377. doi:10.1039/C5CS00118H.

[19] F. Reessing, W. Szymanski, Beyond Photodynamic Therapy: Light-Activated Cancer Chemotherapy, Curr. Med. Chem. 24 (2017) 4905–4950.

[20] R. Horbert, B. Pinchuk, P. Davies, D. Alessi, C. Peifer, Photoactivatable Prodrugs of Antimelanoma Agent Vemurafenib, ACS Chem. Biol. 10 (2015) 2099–2107. doi:10.1021/acschembio.5b00174.

[21] W. Szymanski, J.M. Beierle, H.A. V Kistemaker, W.A. Velema, B.L. Feringa, Reversible Photocontrol of Biological Systems by the incorporation of molecular photoswitches, Chem. Rev. 113 (2013) 6114–6178. doi:10.1021/cr300179f.

[22] C. Brown, S.K. Rastogi, S.L. Barrett, H.E. Anderson, E. Twichell, S. Gralinski, A. Mcdonald, W.J. Brittain, Journal of Photochemistry and Photobiology A : Chemistry Differential azobenzene solubility increases equilibrium cis / trans ratio in water, J. Photochem. Photobiol. 336 (2017) 140–145.

[23] W. Szymanski, M.E. Ourailidou, W.A. Velema, F.J. Dekker, B.L. Feringa, Light-Controlled Histone Deacetylase (HDAC) Inhibitors: Towards Photopharmacological Chemotherapy, Chem. Eur. J. 21 (2015) 16517–16524.

[24] M.J. Hansen, W.A. Velema, G. de Bruin, H.S. Overkleeft, W. Szymanski, B.L. Feringa, Proteasome inhibitors with photocontrolled activity, Chembiochem. 15 (2014) 2053–2057. doi:10.1002/cbic.201402237.

[25] B. Blanco, K.A. Palasis, A. Adwal, D.F. Callen, A.D. Abell, Azobenzene-containing photoswitchable proteasome inhibitors with selective activity and cellular toxicity, Bioorganic Med. Chem. 25 (2017) 5050–5054. doi:10.1016/j.bmc.2017.06.011.

[26] A.J. Engdahl, E.A. Torres, S.E. Lock, T.B. Engdahl, P.S. Mertz, C.N. Streu, Synthesis, Characterization, and Bioactivity of the Photoisomerizable Tubulin Polymerization Inhibitor azo-Combretastatin A4, Org. Lett. 4 (2015) 4546–4549.

[27] M. Borowiak, W. Nahaboo, M. Reynders, K. Nekolla, P. Jalinot, J. Hasserodt, M. Rehberg, M. Delattre, S. Zahler, A. Vollmar, D. Trauner, O. Thorn-seshold, Photoswitchable Inhibitors of Microtubule Dynamics Optically Control Mitosis and Cell Death, Cell. 162 (2015) 403–411.

[28] J.E. Sheldon, M.M. Dcona, C.E. Lyons, J.C. Hackett, M.C.T. Hartman, Photoswitchable Anticancer Activity via trans-cis Isomerization of a Combretastatin A-4 Analog, Org. Biomol. Chem. 14 (2016) 40–49.

[29] S.K. Rastogi, Z. Zhao, S.L. Barrett, S.D. Shelton, M. Zafferani, H.E. Anderson, M.O. Blumenthal, L.R. Jones, L. Wang, X. Li, C.N. Streu, L. Du, W.J. Brittain, Photoresponsive azo-combretastatin A-4 analogues, Eur. J. Med. Chem. 143 (2018)

1–7. https://doi.org/10.1016/j.ejmech.2017.11.012.

[30] R. Ferreira, J.R. Nilsson, C. Solano, J. Andréasson, M. Grøtli, Design , Synthesis and Inhibitory Activity of Photoswitchable RET Kinase Inhibitors, Sci. Rep. 5 (2015) 9769.

[31] D. Wilson, J.W. Li, N.R. Branda, Visible-Light-Triggered Activation of a Protein Kinase Inhibitor, (2017) 1–5. doi:10.1002/cmdc.201600632.

[32] D. Schmidt, T. Rodat, L. Heintze, J. Weber, R. Horbert, U. Girreser, T. Raeker, L. Bußmann, M. Kriegs, B. Hartke, C. Peifer, Axitinib - A Photoswitchable Approved Tyrosine Kinase Inhibitor., ChemMedChem. (2018). doi:10.1002/cmdc.201800531.

[33] C.L. Fleming, M. Grøtli, J. Andreasson, On-Command Regulation of Kinase Activity using Photonic Stimuli, ChemPhotoChem. (2019). doi:10.1002/cptc.201800253.

[34] M. Schehr, C. Ianes, J. Weisner, L. Heintze, M.P. Müller, C. Pichlo, J. Charl, E. Brunstein, J. Ewert, M. Lehr, U. Baumann, D. Rauh, U. Knippschild, C. Peifer, R. Herges, 2-Azo-, 2-diazocine-thiazols and 2-azo-imidazoles as photoswitchable kinase inhibitors: limitations and pitfalls of the photoswitchable inhibitor approach, Photochem. Photobiol. Sci. DOI: 10.10 (2019). doi:10.1039/c9pp00010k.

[35] S. Wenglowsky, D. Moreno, E.R. Laird, S.L. Gloor, L. Ren, T. Risom, J. Rudolph, H.L. Sturgis, W.C. Voegtli, Pyrazolopyridine inhibitors of B-RafV600E. Part 4: Rational design and kinase selectivity profile of cell potent type II inhibitors, Bioorganic Med. Chem. Lett. 22 (2012) 6237–6241. doi:10.1016/j.bmcl.2012.08.007.

[36] B.J. Newhouse, S. Wenglowsky, J. Grina, E.R. Laird, W.C. Voegtli, L. Ren, K. Ahrendt, A. Buckmelter, S.L. Gloor, N. Klopfenstein, J. Rudolph, Z. Wen, X. Li, B. Feng, Imidazo[4,5-b]pyridine inhibitors of B-Raf kinase, Bioorganic Med. Chem. Lett. 23 (2013) 5896–5899. doi:10.1016/j.bmcl.2013.08.086.

[37] S. Wenglowsky, L. Ren, J. Grina, J.D. Hansen, E.R. Laird, D. Moreno, V. Dinkel, S.L. Gloor, G. Hastings, S. Rana, K. Rasor, H.L. Sturgis, W.C. Voegtli, G. Vigers, B. Willis, S. Mathieu, J. Rudolph, Highly potent and selective 3-N-methylquinazoline-4(3H)-one based inhibitors of B-RafV600Ekinase, Bioorganic Med. Chem. Lett. 24 (2014) 1923–1927. doi:10.1016/j.bmcl.2014.03.007.

[38] M. Pulici, G. Traquandi, C. Marchionni, M. Modugno, R. Lupi, N. Amboldi, E. Casale, N. Colombo, L. Corti, M. Fasolini, F. Gasparri, W. Pastori, A. Scolaro, D. Donati, E. Felder, A. Galvani, A. Isacchi, E. Pesenti, M. Ciomei, Optimization of diarylthiazole B-Raf inhibitors: Identification of a compound endowed with high oral antitumor activity, mitigated hERG inhibition, and low paradoxical effect, ChemMedChem. 10 (2015) 276–295. doi:10.1002/cmdc.201402424.

[39] L. Liu, M.R. Lee, J.L. Kim, D.A. Whittington, H. Bregman, Z. Hua, R.T. Lewis, M.W. Martin, N. Nishimura, M. Potashman, K. Yang, S. Yi, K.R. Vaida, L.F. Epstein, C. Babij, M. Fernando, J. Carnahan, M.H. Norman, Purinylpyridinylamino-based DFG-in/αC-helix-out B-Raf inhibitors: Applying mutant versus wild-type B-Raf selectivity indices for compound profiling, Bioorganic Med. Chem. 24 (2016) 2215–2234. doi:10.1016/j.bmc.2016.03.055.

[40] I.C. Waizenegger, A. Baum, S. Steurer, H. Stadtmu ller, G. Bader, O. Schaaf, P. Garin-Chesa, A. Schlattl, N. Schweifer, C. Haslinger, F. Colbatzky, S. Mousa, A. Kalkuhl, N. Kraut, G.R. Adolf, A Novel RAF Kinase Inhibitor with DFG-Out-Binding Mode: High Efficacy in BRAF-Mutant Tumor Xenograft Models in the Absence of Normal Tissue Hyperproliferation, Mol. Cancer Ther. 15 (2016) 354–365. doi:10.1158/1535-7163.MCT-15-0617.

[41] M. Schoenberger, A. Damijonaitis, Z. Zhang, D. Nagel, D. Trauner, Development of a

New Photochromic Ion Channel Blocker via Azologization of Fomocaine, ACS Chem. Neurosci. 5 (2014) 514–518.

[42] B. Pinchuk, T. Von Drathen, V. Opel, C. Peifer, Photoinduced Conversion of Antimelanoma Agent Dabrafenib to a Novel Fluorescent BRAFV600E Inhibitor, ACS Med. Chem. Lett. 7 (2016) 962–966. doi:10.1021/acsmedchemlett.6b00340.

[43] S. Wenglowsky, K.A. Ahrendt, A.J. Buckmelter, B. Feng, S.L. Gloor, S. Gradl, J. Grina, J.D. Hansen, E.R. Laird, P. Lunghofer, S. Mathieu, D. Moreno, B. Newhouse, L. Ren, T. Risom, J. Rudolph, J. Seo, H.L. Sturgis, W.C. Voegtli, Z. Wen, Pyrazolopyridine inhibitors of B-RafV600E. Part 2: Structure-activity relationships, Bioorganic Med. Chem. Lett. 21 (2011) 5533–5537. doi:10.1016/j.bmcl.2011.06.097.

[44] W. Szymanski, B. Wu, C. Poloni, D.B. Janssen, B.L. Feringa, Azobenzene photoswitches for staudinger-bertozzi ligation, Angew. Chem. Int. Ed. 52 (2013) 2068–2072.

[45] M. Matsuse, N. Mitsutake, S. Tanimura, T. Ogi, E. Nishihara, M. Hirokawa, C.S. Fuziwara, V.A. Saenko, K. Suzuki, A. Miyauchi, S. Yamashita, Functional characterization of the novel BRAF complex mutation, BRAFV600delinsYM, identified in papillary thyroid carcinoma, Int. J. Cancer. 132 (2013) 738–743. doi:10.1002/ijc.27709.

[46] M. Hatanaka, Y. Higashi, K. Kawai, J. Su, W. Zeng, X. Chen, T. Kanekura, CD147-targeted siRNA in A375 malignant melanoma cells induces the phosphorylation of EGFR and downregulates CDC25C and MEK phosphorylation, Oncol. Lett. 11 (2016) 2424–2428. doi:10.3892/ol.2016.4267.

[47] O. Hantschel, Unexpected off-targets and paradoxical pathway activation by kinase inhibitors, ACS Chem. Biol. 10 (2015) 234–245. doi:10.1021/cb500886n.

[48] A. Ter Elst, S.H. Diks, K.R. Kampen, P.M. Hoogerbrugge, R. Ruijtenbeek, P.J. Boender, A.H. Sikkema, F.J.G. Scherpen, W.A. Kamps, M.P. Peppelenbosch, E.S.J.M. De Bont, Identification of new possible targets for leukemia treatment by kinase activity profiling, Leuk. Lymphoma. 52 (2011) 122–130. doi:10.3109/10428194.2010.535181.

[49] A.H. Ree, K. Flatmark, M.G. Saelen, S. Folkvord, S. Dueland, J. Geisler, K.R. Redalen, Tumor phosphatidylinositol 3-kinase signaling in therapy resistance and metastatic dissemination of rectal cancer: Opportunities for signaling-adapted therapies, Crit. Rev. Oncol. Hematol. 95 (2015) 114–124. doi:10.1016/j.critrevonc.2015.01.003.

[50] E. Baron, S. Stevens, Phototherapy for cutaneous T-cell lymphoma, Dermatol. Ther. 16 (2003) 303–310.

[51] M.W.H. Hoorens, W. Szymanski, Reversible, Spatial and Temporal Control over Protein Activity Using Light, Trends Biochem. Sci. 43 (2018) 567–575. doi:10.1016/j.tibs.2018.05.004.

[52] M. Wang, M. Gao, K.D. Miller, Q. Zheng, Synthesis of 2,6-difluoro-N-(3-[11C]methoxy-1H-pyrazolo[3,4-b]pyridine-5-yl)-3-(propylsulfonamidio)benzamide as a new potential PET agent for imaging of B-RAFV600E in cancers, Bioorg. Med. Chem. Lett. 23 (2013) 1017–1021. doi:10.1016/j.bmcl.2012.12.027.

[53] A. Jankowiak, E. Obijalska, P. Kaszynski, A. Pieczonka, V.G. Young, Synthesis and structural, spectroscopic, and electrochemical characterization of benzo[c]quinolizinium and its 5-aza, 6-aza, and 5, 6-diaza analogues, Tetrahedron. 67 (2011) 3317–3327. doi:10.1016/j.tet.2011.03.023.